AN ON-LINE

MEASUREMENT OF RESIDENCE TIME DISTRIBUTION

IN A TWIN-SCREW EXTRUDER

by
Tong Chen
Department of Chemical Engineering
McGill University
Montreal
January, 1992

A Thesis submitted to
the Faculty of Graduate Studies and Research in
partial fulfilment of the requirement of the
degree of Master of Engineering

ABSTRACT

The importance of the residence time distribution (RTD) in polymer extrusion has been recognized for a long time, however, it is very difficult to measure. In this project, an optical on-line RTD measurement technique based on extrudate transmittance changes was investigated. A He-Ne laser beam was the light source, and carbon black was the tracer and detection was performed by a photomultiplier.

The RTD of a ZSK-30 twin-screw extruder was measured with and without an in-line rheometer installed. Various operating conditions were used to examine their effects on the RTD curve. It was found that the mean residence time of the system decreased linearly with screw speed and exponentially with the feed rate. The temperature effect was minuscule. The in-line rheometer increased the mean residence time of the system by 80%.

RÉSUMÉ

Depuis longtemps l'importance de la distribution du temps de séjour a été mise en évidence pour le procédé d'extrusion des thermoplastiques. Cette dernière est cependant trés difficile à mesurer. Dans ce projet, une méthode optique de mesure en simultené de la distribution du temps de séjour est étudiée en suivant l'évolution de la transmittance du produit extrudé. Un faisceau laser He-Ne est utilisé comme source lumineuse, le traceur est du noir de carbone, et la detection est realisée à l'aide d'un photomultiplicateur.

La distribution du temps de séjour d'une extrudeuse ZSK-30 est mesurée avec cette technique, avec et sans rhéomètre en ligne. L'effet de diverses conditions d'opération sur les courbes de distribution du temps de séjour est examiné. La durée moyenne de séjour dans le système décroit linéairement avec la vitesse de rotation de la vis, et exponentiellement avec la vitesse d'alimentation. L'effet de la température est négligeable. Le rhéomètre en ligne augmente la durée moyenne de séjour du système de 80%.

ACKNOWLEDGEMENTS

I would like to express my sincere thanks to following people for their support during the research for and in the preparation of my thesis:

——— My research directors, Prof. J.M. Dealy and Prof. W.I. Patterson for initiating me into the field of polymer processing, pushing and encouraging me throughout the course of this project, and for their critical review of this thesis.

——— My colleagues Mr T.O. Broadhead and Mr B.I. Nelson for their advice in the ZSK-30 extruder operating and troubleshooting, and for their helpful discussions of various kinds of problems.

——— Mr A. Krish, Mr J. Dumont and the staff of the Chemical Engineering machine shop for their assistance in equipment procurement, fabrication and installation.

——— Members of the Magnetic Materials Group of the McGill Physics Department for providing the ferromagnetic fibres.

TABLE OF CONTENTS

CHAPTER 1 INTRODUCTION

Extrusion is an important, fundamental polymer processing operation, and extruders are widely used in the plastics, rubber and fibre industries. A broad range of polymer systems are commercially extruded ranging from homogeneous melts to systems with suspended solid particles, two-phase melt systems and foams. While single screw extruders are easy to design and can have high throughput, twin-screw extruders can control their mixing performance. The modular co-rotating twin-screw extruder, such as the ZSK- series made by Werner & Pfleiderer, is one of the more important types of processing machinery, and is used as a chemical reactor, devolatilizer, and compounder throughout the polymer industry to achieve improved dispersing and mixing.

The measurement and analysis of the residence time distribution (RTD) of a unit operation is an important tool in the study of continuous systems. This is especially true for the reactive extrusion process where reaction time has a great impact on the product quality. RTD knowledge can be used to describe mixing, flow patterns, conversion, and product quality. Historically, the RTD was first used to describe chemical reactors, but this concept is now finding application in a variety of unit operations, including extrusion. A knowledge of the RTD is very important to process and quality control. Applications in the polymer processing industry

include: the mixing of additives and fillers with polymer, controlled degradation during processing, and devolatilization. Residence time distribution research in polymer processing has been focused on extrusion because of its wide use and versatility.

In this chapter, a brief review of extrusion and extruders and a survey of previous work is given, followed by the objectives of this project.

1.1 Extrusion And Extruders

The extrusion process, as described in many books (12,18, 20,22,25,29,35,36,37), is basically a melting, mixing and pumping process. An extruder is composed of one (or more) motor-driven screw(s) rotating inside a barrel with heating and cooling facilities. Polymer resin and other additives are fed at one end through a hopper, melted and sheared by the rotating screw, and forced out under pressure at the other end through a die. The objective of the process is to produce a homogeneous molten material at a certain flow rate, pressure, and temperature, ready for the next operation in the process line.

The basic method of analyzing the mixing and pumping processes in an extruder involves the following steps: for given screw geometry, write the basic continuum mechanics equations and the rheological constitutive equation for the molten polymer, make some assumptions to simplify these

equations, and then solve them either analytically or numerically to yield relations between the variables of interest. This is the fundamental mathematical modelling procedure.

A single screw extruder is basically a screw pump. It can be modelled by solving the fluid mechanics and constitutive equations for the molten polymer inside an "unwound" finite length shallow channel covered with an infinite moving plate (Figure 1.1).

For twin-screw extruders, however, modelling is more difficult (for example see Refs.11,13,19,46). Twin-screw extruders come in a variety of configurations and arrangements. The screws can be co-rotating or counter-rotating, they can be non-, partially, or fully inter-meshing, or have other geometrical distinctions (8,27,42) such as mixing sections. The infinite rectangular channel model is no longer valid. The intermeshing of the two screws has the effect of breaking up the helical channels on each screw into a series of largely independent, C-shaped volumes or chambers as illustrated in Figure 1.2. By assuming very little leakage flow, Tadmor and Gogos (1970) developed a plate and frame model to describe polymer pumping and mixing in the C-chambers. However, it is known that only fully intermeshing counter-rotating screws can form truly positive displacement pumps (36). In the co-rotating case, the leakage flow is generally significant. The special geometries designed for kneading and self-wiping make analysis more complicated.

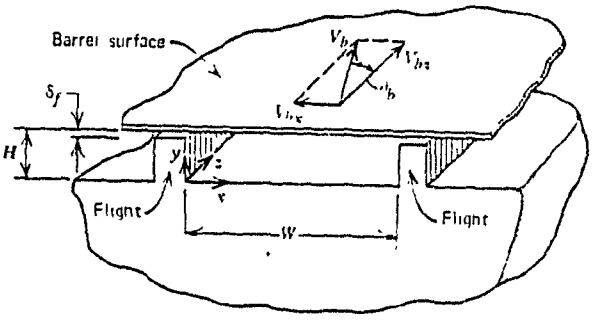

Figure 1.1 Geometry of the "unwound" rectangular channel

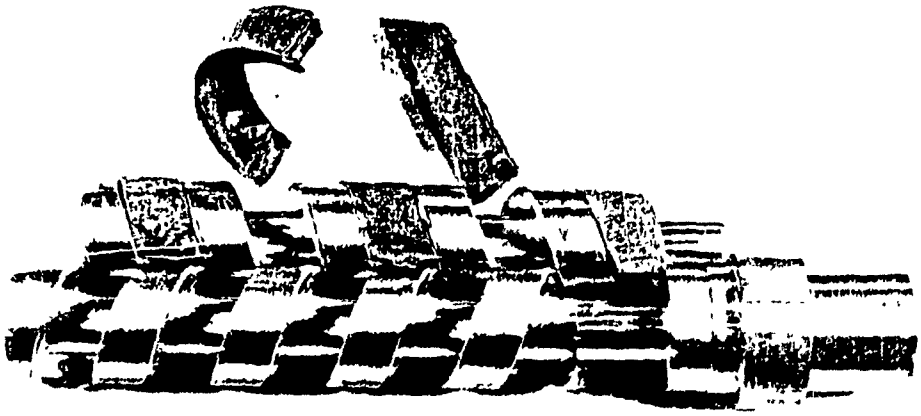

Figure 1.2 C-chambers in screws of a counter-rotating extruder

(Figure 1.1 & 1.2 are quoted from reference 36)

Thus, dealing with a non-Newtonian polymer melt, a complex screw structure and normally starve-fed operating conditions, it has proved impossible to calculate analytically the flow inside a twin-screw extruder.

1.2 Importance of Residence Time Distribution (RTD)

The elaborate screw structure and various possible arrangements make it too complicated to develop a detailed model for a twin-screw extruder. Therefore, experimental tests become essential to characterize the performance of twin-screw extruders. Among possible measurements, the residence time distribution (RTD) plays a special role. The RTD describes the time history of the polymer inside the extruder. Knowledge of the RTD is thus important to understand continuous reactive engineering processes taking place in a twin-screw extruder.

Generally, the time the material spends in the extruder will be reflected in the quality of the product, degree of mixing, efficiency of chemical reaction and extent of degradation. For normal polymer extrusion the shape of the RTD tells us how long a certain portion of the material is exposed to the extrusion heat load and shearing action. A combination of this thermal load and shear and the time of exposure gives an indication of the possible degradation or other reaction such as cross-linking. When an extruder is used as a chemical reactor, the molecular weight distribution of the product is strongly affected by the breadth of the RTD. A recent study of

the degradation of high density polyethylene (HDPE) using RTD analyses was reported by Dontula et al.(1991).

1.3 Previous Work on Extruder Modelling and RTD Measurement

The studies on the performance of extruders have been, since the beginning, included RTD measurements.

The earliest modelling of a single screw extruder dates from 1953 to 1962 when Mohr et al.(1957) and McKelvey (1962) derived expressions for the strain distribution in the isothermal flow of a Newtonian fluid by modelling the screw geometry as fully-filled straight rectangular channels. They also introduced, for the first time, the concept of the RTD to describe the polymer extrusion process. Later, Pinto and Tadmor (1970) and Tadmor and Klein (1970) further developed this model for melt extrusion. They derived a formula for calculating the RTD and then used a RTD-weighted total strain as a quantitative criterion to describe the goodness of mixing in an extruder.

Three other models for single screw extruder are not based directly on the screw geometry but start from the idea of the overall system transfer function. These models are adopted from three RTD models of general chemical processes. The one developed by Wolf and Resnick (1963) for various non-ideal flow systems was based on the idea of a "modified perfect mixing flow", and the two developed by Levenspiel (1972) were based on the idea of "tanks in series" and "an

axial dispersion superimposed on a plug flow". The mathematical expressions for all three models are expressed in terms of the RTD.

There are many modifications of these models for single screw extruders, developed to suit a specific extruder and polymer.

For twin-screw extruders, although these are being used more and more in industry, knowledge of the flow phenomena that occur in these machines is still poor (42). Due to their complex configuration and the variety of screw arrangements (for modular screws), the techniques used to model single screw extruders are very difficult to apply.

By assuming isothermal flow of a Newtonian fluid and that the mixing chamber is fully filled, White (1990) tried to derive the flow and mixing characteristics for a modular, intermeshing co-rotating, twin-screw extruder. He first derived the characteristic curves for all the screw elements, and then used these curves together with the measured throughput and pressure to calculate the flow rate and the degree of mixing. Taking advantage of modern computational techniques, Gotsis and Kalyon (1989) carried out a simulation of mixing in a co-rotating extruder by applying a finite element method to different regions of that extruder. Tedious calculations can be avoided by employing an experimental visual method. Bigio and Wigginton (1990) recently reported on an experimental study of the mixing process in a counter-rotating, non-

intermeshing extruder.

Nevertheless, many of the flow and mixing studies on twin-screw extruders were carried out using the RTD concept, and most of them directly relied on experimental RTD measurements. Potente and Schultheis (1989), for instance, calculated the minimum and mean residence times from the screw structure and the operating conditions and used only these two variables to calculate the RTD function and to model the mixing of the counter-rotating extruder. At the same time, an experimental RTD measurement was carried out in order to test the validity of their model. Bounie (1983), on the other hand, made experimental measurements of the RTD for a co-rotating twin-screw extruder first, and then modeled the flow pattern for that extruder by frequency domain curve fitting to the experimental RTD result.

The development of tracer-sensor techniques led to more experimental measurements of the RTD in twin-screw extruders in the past decade. Most of these were discontinuous measurements, i.e., discrete extrudate samples were collected in time sequence, and then the tracer concentrations in these samples were measured in the laboratory (for example see Refs.2,3,5,7, 14,15,28,38).

A continuous, or on-line, measurement technique was first developed by Wolf and White (1976) for the study of a single screw extruder. Golba (1980) and Bur et al.(1990) continuously measured the RTD on co-rotating twin-screw extruders. Recent-

ly, Sakai and Hashimoto (1990) and Schule et al.(1988) performed on-line RTD measurements on both counter- and co-rotating extruders using different techniques. The advantages of on-line measurement include not only the elimination of the laborious and time-consuming taking of extrudate samples and subsequent evaluation, but also the providing of a more complete and accurate RTD curve that makes it possible to check the incorporation of the tracer and the mixing of the screws. Integration of the area under a continuous RTD curve gives the overall tracer mass balance.

1.4 Project Objectives

Until now there have been no satisfactory studies of RTD and mixing in intermeshing co-rotating twin-screw extruders (42). A direct measurement of the RTD for a specific extruder was desired. A Werner & Pfleiderer ZSK-30 co-rotating, intermeshing twin-screw extruder is installed at McGill. It was used by Nelson (1992) and Broadhead (1992) to develop an in-line rheometer and to use it for the closed-loop control of reactive extrusion processes. A knowledge of the RTD of this machine will be very helpful to understand and ultimately improve the control of that system.

This project consists of an experimental RTD measurement. The primary objectives of the project were:

1. To examine methods of on-line RTD measurement either by using a ferro-magnetic powder as the tracer, and

measuring the magnetic inductance of the extrudate or, by using carbon black as the tracer, and measuring the optical transmittance of the extrudate.

2. To measure the tracer distribution in the extrudate of the ZSK-30 twin-screw extruder using one of the techniques investigated.

The secondary objectives of this project were:

3. To study the dependence of the RTD on the feed rate and the screw speed.

4. To investigate the RTD curves obtained with and without the in-line rheometer installed, the purpose being to facilitate the evaluation of the dynamic response of the in-line rheometer.

The following chapters describe the background, methodology and the results of this project. Chapter 2 provides a background knowledge about RTD and its determination and a survey of the relevant research reported in the literature. Chapter 3 discusses three methods commonly used for RTD measurement. Chapter 4 describes the hardware, the interface, and the methodology developed during the course of this work. Chapter 5 presents the results obtained and a discussion of these results. The conclusions and recommendations for future work are given in Chapter 6.

CHAPTER 2 BACKGROUND

A general definition of mixing is that it is a time-dependent process that removes composition inhomogeneity existing in three-dimensional space. This is spatial mixing. This definition is adequate for the mixing that occurs in a batch process. For a continuous flow system, however, fluid elements have an attribute that is not strictly compositional but can also be used to characterize mixing. This attribute is called age, which is the time that the fluid element has spent in the system. For a continuous process at steady state, the composition at a point never changes, but individual particles moving through the system may experience many different environments and mix with particles having many different ages. This is the concept of time mixing. Both these mixing concepts have been discussed by Nauman and Buffham (1983).

The characterization of mixing in terms of ages allows a treatment of continuous flow systems. This treatment is independent of specific mixing mechanisms, and it is thus very useful for the twin-screw extruder system, which has a complex structure.

2.1 RTD and Mixing

The age of a particle, measured from its entrance to the system to its final departure from the system, is called the exit age of that particle or the residence time, t. The term "particle" here means any small entity that is conserved when

passing through the system.

2.1.1 Residence Time Distribution Functions

The population of particles falling into different residence time intervals form a continuous distribution curve, as illustrated in Figure 2.1.

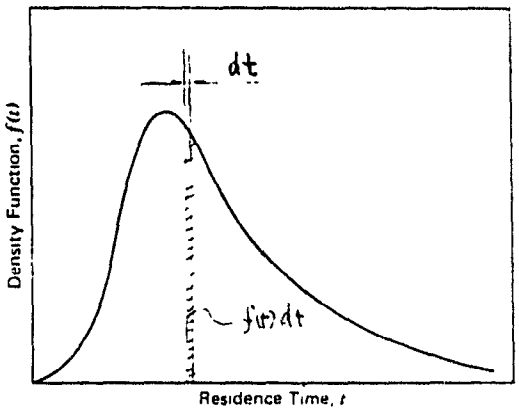

Figure 2.1 Residence time density function

Here, f(t)dt denotes the probability that the residence time is in the interval (t,t+dt), while f(t) is a function of residence time that characterizes the nature of the mixing in a flow system. The function f(t) is called the "residence time density function" or "residence time distribution function (RTD)". It has the property:

$$\int_0^\infty f(t)\,dt = 1 \qquad (2.1)$$

since the possible different residence times are mutually exclusive.

There are other ways to describe the RTD of a system. Among them, the most commonly used are:

(1). The cumulative distribution function, F(t), defined

as the probability that a particle has a residence time less than t.

$$F(t) = \int_0^t f(\tau)\,d\tau \qquad (2.2)$$

(2). The washout function, W(t), defined as the probability that a particle has a residence time greater then t.

$$W(t) = \int_t^\infty f(\tau)\,d\tau \qquad (2.3)$$

2.1.2 Mean Residence Time and Normalized RTD

Moments are often used to mathematically characterize a distribution function. The first order moment of a RTD function is specially important in our case. It has a physical meaning as the mean residence time (particulate mean)

$$\bar{t} = \mu_1 = \int_0^\infty t\,f(t)\,dt \qquad (2.4)$$

For incompressible fluids in closed systems, Danckwerts (1953) and Zwietering (1959) showed that

$$\bar{t} = \frac{V}{Q} \qquad (2.5)$$

where V is the effective volume (hold-up) of the system, and Q is the volumetric flow rate.

By using a dimensionless time $\theta = t/\bar{t}$, we can write a normalized (dimensionless) RTD function $f_\theta(\theta)$.

It is easy to show that:

$$f_\theta = \bar{t} f \qquad (2.6)$$

It is more convenient to use the normalized RTD function to compare the mixing between processes having different mean residence times.

2.1.3 Mixing and RTD Curves

There are two extreme cases of mixing: plug flow (where there is no mixing), and perfect mixing (where there is no inhomogeneity in space). The former gives

$$f(t) = \delta(t-\bar{t}) \quad or \quad f_\theta(\theta) = \bar{t}\,\delta(\theta-1) \qquad (2.7)$$

while the latter gives

$$f(t) = \frac{1}{\bar{t}} e^{-\frac{t}{\bar{t}}} \quad or \quad f_\theta(\theta) = e^{-\theta} \qquad (2.8)$$

A real process is neither of these two but always lies between the extremes.

The normalized RTD curve reveals the mixing extent of a process. For the dispersion model given by Levenspiel (1972) for example, the vessel dispersion number D/uL (for a closed vessel, u is the flow velocity, L is the vessel length, and D is the axial dispersion coefficient), is directly linked with the shape of the RTD curve. This is illustrated in Figure 2.2. If the dispersion number is small, the normalized RTD curve is nearly symmetric, and the dispersion number can be directly determined from it (see Figure 2.3).

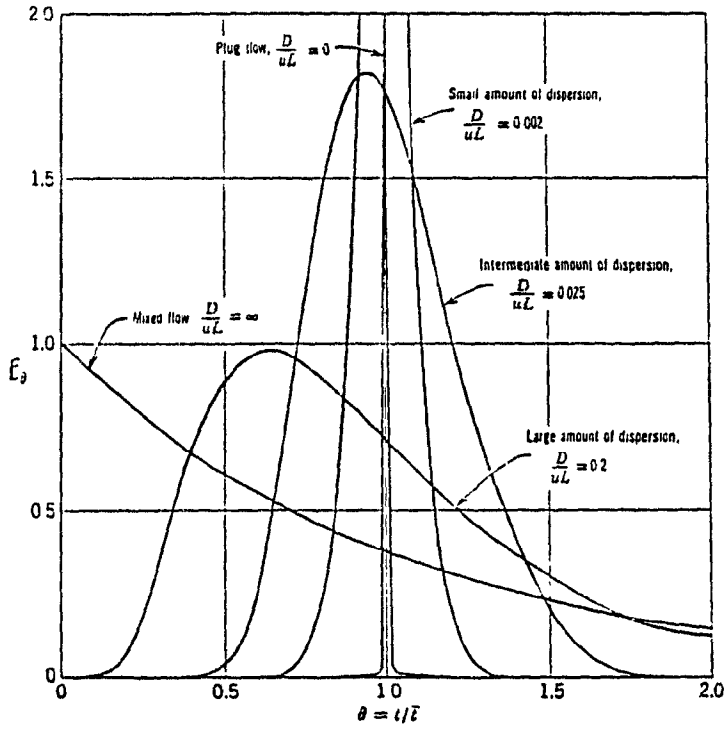

Figure 2.2 Normalized RTD curves for various extent of back-mixing as predicted by the dispersion model

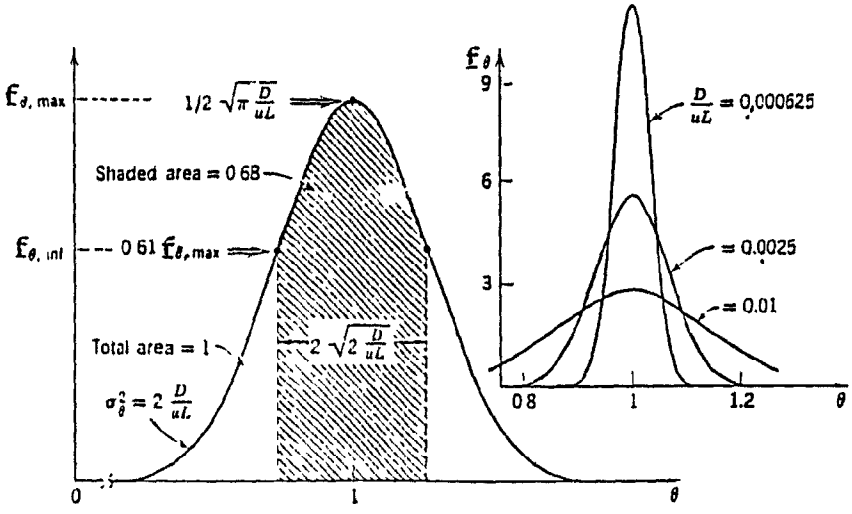

Figure 2.3 Relationship between D/uL and the normalized dimensionless RTD curve for small extent of dispersion

(Figure 2.2 and 2.3 are from Levenspiel (1972))

2.2 Experimental Determination of RTD

From the previous discussion it is clear that the RTD curves are directly linked with the extent of mixing. To determine the RTD function for a continuous flow system, some tracer particles are introduced at the inlet and later collected in time sequence at the outlet. The input concentration of the tracer $C_{in}(t)$ is known, and the output concentration $C_{out}(t)$ is measured. For an arbitrary input tracer concentration $C_{in}(t)$, the output concentration will be

$$C_{out}(t) = C_{in}(t) * f(t) \qquad (2.9)$$

where * denotes convolution.

Thus by knowing $C_{out}(t)$ and $C_{in}(t)$ the residence time distribution function of the system can be determined.

The most common choices for the input function $C_{in}(t)$ are the step and the impulse functions, because they lead to simple and straightforward relations between the measured variable $C_{out}(t)$ and the function f(t). These are discussed in the following two sections.

2.2.1 Step-change Responses

For a positive step change input of magnitude $C_{in}(t>0)=C_0$, from Eq.2.9 we can derive:

$$C_{out}(t) = C_0 \int_0^t f(\tau)\, d\tau \qquad (2.10)$$

Thus from Eq.2.2 we have:

$$C_{out}(t) = C_0 F(t) \quad or \quad F(t) = \frac{C_{out}(t)}{C_0} = \frac{C_{out}(t)}{C_{out}(\infty)} \tag{2.11}$$

Similarly, for a negative step change from an original concentration $C_{in}(t<0)=C_0$ to $C_{in}(t>0)=0$, the system response will be

$$C_{out} = C_0 W(t) \quad or \quad W(t) = \frac{C_{out}(t)}{C_{out}(0)} \tag{2.12}$$

Positive step change experiments lead directly to the cumulative distributive function F(t), while a negative step change leads to the washout function W(t). Both of these have been used in RTD measurement experiments (9,28). The negative step change provides the best possible method for defining the tail of the distribution, since a value of $C_{out}(\infty)$ is not needed in Eq.2.12. For step change methods, the absolute tracer concentration needed is lower than that for the impulse method, so tracer diffusion is less important.

The disadvantages of these methods are that they consume a lot of tracer material and sometimes it is not easy to provide a perfect step change.

2.2.2 Impulse Response

The impulse technique approximates a Dirac (or impulse) input function by injecting into the inlet some high concentration tracer within a very short time period. If we let C_0 be the weight percent concentration of the tracer, and neglect the effect of the injection on the flow rate, it is easy to

show that

$$C_{in}(t) = \frac{WC_0}{Q\Delta t} \qquad (2.13)$$

where Q is the volumetric flow rate, W is the total tracer amount injected, and Δt is the injection time when the pulse exists.

From Eq.2.13 it is clear that only in the extreme case where C_0=100% and $\Delta t \to 0$ is a perfect impulse formed:

$$\frac{C_{in}(t)\,Q}{W} = \delta(t) \qquad (2.14)$$

For this perfect impulse input, the system's output will be, according to Eq.2.9,

$$f(t) = \frac{Q}{W} C_{out}(t) \qquad (2.15)$$

The RTD function is thus directly determined by measuring the output concentration.

For a discrete system, $W \approx \Sigma Q C_{out}(t_i) T$, where T is the sampling period, Eq.2.15 becomes

$$f(t_i) = \frac{C_{out}(t_i)}{\sum_0^\infty C_{out}(t_i)\,T} \qquad (2.16)$$

2.3 Tracer Characteristics and Concentration Detection

The proper choice of tracer is fundamental for a successful stimulus-response test. A tracer must be both mechanically and chemically stable under the operating conditions. Generally there are two criteria for a good

tracer. First, it must have flow properties similar to the working polymer. Thus, the injection of this tracer will not affect the mixing and pumping processes, and hence the stimulus-response results based on the tracer concentration will reflect the true RTD. Second, it must be "visible" throughout the extrudate, i.e., it must be easily detected in the working polymer. These two criteria are somewhat contradictory. However, under certain circumstances it is possible to find a tracer suitable for a given extrusion process.

The second criterion leads us to seek a material that has a distinguishable characteristic (other than flow characteristic) significantly different from that in the processing material. Usually these characteristics are: colour or opacity, electronic property, magnetic property, or radioactivity. The first criterion limits the particle size of the tracer, the amount injected and normally leads to a doping technique for the tracer in the working polymer (some times called a master-batch).

Guided by these rules, various tracer/detector techniques have been developed for different systems. Bigg and Middleman (1974) used a red food dye in an aqueous solution of polyacrylamide and measured its concentration by means of a light transmittance spectrometer. Stamato and Weiss (1985) worked with polystyrene (PS). They marked the polymer by introducing an ionic group onto it, and coloured the collected extrudate samples with a counterion dye. Dontula et al.(1991) used

cobalt blue with a high density polyethylene (HDPE) system and detected it by means of a colorimeter. Golba (1980) used carbon-black in PS and made on-line measurements of the dielectric constant of the extrudate. Schule et al.(1988) adopted an inductive measuring technique using iron power as a tracer in a HDPE system. A radioactive tracer technique was first used by Wolf and White (1976) with a polyethylene (PE) system, and this technique was later used by Janssen et al.(1979) and by Tzoganakis (1989) with polypropylene (PP). Both used $^{56}MnO_2$ as the tracer material.

Kao and Allison (1984) tried both a yellow dye and carbon black pigment with a styrene-based copolymer. They reported that there was no significant difference between results obtained using these two tracers. Potente and Lappe (1986) also tried different tracers including a soluble dye, a pigment, and glass spheres with different diameters, with a PE system. They found, however, that the RTD curves became flatter with increasing tracer particle diameter. They concluded that only a soluble dye can be used to get a true RTD. Details of the techniques were not published, and we can not make any comment about these arguments. We note, however, that Potente and Lappe worked on a single-screw extruder while Kao and Allison worked on a ZSK-30 twin-screw extruder.

Recently, Cassagnau et al.(1991) made RTD measurements with a polyvinyl chloride (PVC) system using grafted phenyl and anthracene as tracer materials. They believed that even a

soluble dye is not good enough to get the true RTD. Perhaps this is somewhat exaggerated since the time-consuming extrudate sampling procedure, the rather completed pre-treatment of these samples before measuring, the reliability of the detecting technique, and finally the sensitivity and stability of the measuring instrument may all together cause an error greater than the small variations of the RTD curve caused by the tracer itself.

When an on-line measurement is required, it is necessary to develop a suitable sensor to detect the tracer concentration continuously under working conditions. The tracer system must be "visible" by that sensor which must have a large and reproducible response to changes in concentration. The detection system must be sensitive, precise, stable, able to withstand the service conditions of the process environment, and easily calibrated. An automatic data acquisition system is also desirable.

Although people have tried and are still trying hard to improve the on-line measuring technique, up to now it is still far from perfect.

CHAPTER 3 METHODS FOR MEASURING THE RTD

Various detecting techniques have been developed corresponding to different tracer properties. Among these are three methods often used for RTD measurement: the radioactive tracer method, the electrical/magnetic tracer method, and the optical method. Both the magnetic and optical methods were considered for use in this project, but only the optical method was finally used in the on-line RTD measurement experiments because of project time limitations.

3.1 Radioactive Tracer Methods

Radioactive materials can be used as tracers since they are well distinguishable from any kind of polymer. To limit radioactive hazards, fast decaying isotopes are favoured, and these are prepared (irradiated) just before use or collected and irradiated after extrusion.

Without exception, all the reported radioactive RTD measurements (for example see Refs. 14, 40, and 44) involved the use of $^{56}MnO_2$ powder as the tracer material. This is because the $^{56}Mn \rightarrow ^{56}Fe$ decay has a reasonable energy level for detection purposes and a relatively short half-life, about 2.6 hr, which avoids long-term radiation problems. The MnO_2 powder was mixed with the working polymer beforehand to make a tracer master-batch of the desired concentration. For discontinuous RTD measurement, this tracer master-batch was directly

injected, and the extrudate was collected and marked in time sequence. The collected samples were then irradiated with a controlled flux of thermal neutrons. The induced radioactivity of ^{56}Mn decaying to ^{56}Fe was measured for each sample to determine the concentration of MnO_2. For on-line RTD measurement, the tracer master-batch was irradiated before injection, and a scintillation crystal sensor probe was mounted at the extruder outlet monitoring the extrudate radioactivity.

The radioactive method has a high sensitivity and it is easy to cover a tracer concentration range of 3 to 4 orders of magnitude. However, in practical applications, this is limited by the detector system. For off-line measurement, the number of extrudate samples makes it difficult to avoid a flux gradient error when irradiating, and the long time it takes to measure these samples also causes error because of the ongoing decay. For on-line measurement, the sensor must be shielded very carefully to reduce background noise, and the extrudate must be transported immediately. This is a costly, specialized method that was not pursued in the present work.

3.2 Electrical and Magnetic Tracer Methods

Electrical signals are easy to detect and process. Tracers having electrical/magnetic properties far different from working material are used for on-line RTD measurement.

For the polymer extrusion process, it is better to use the dielectric property (capacitance) rather than conduc-

tivity. Golba (1980) developed this method when measuring RTD on a twin-screw extruder with a slit die. The dielectric cell was incorporated into the die, and the capacitance change was continuously monitored to detect the concentration of carbon black (tracer) in polystyrene (working polymer). A similar technique was later used by Nichols et al.(1983). Because the tracer concentrations in the outlet are usually rather low, a very large effective area of the sensor cell (capacitor) is required. This causes some flow disturbance and leads to a sensor error (refer to Appendix 1).

Another alternative is to choose magnetic material as tracer and measure the inductance change upon the outlet stream to determine the tracer concentration. Iron powder is usually chosen as a tracer material since it is cheap, safe, and has a very high relative magnetic permeability (K=3000-5000) compared to polymers (K=1-2). A copper wire coil with non-metallic former is coaxially mounted at the end of the extruder as a sensor monitoring the extrudate passing through. Another coil having the same structure and characteristics is used for zero balancing of the measuring coil. These are linked to a LRC multimeter or a Wheatstone bridge to detect the inductance changes and hence to determine the tracer concentration at the outlet. The most important part of the measuring device is the sensor coil. As illustrated in Figure 3.1, the inductance of such a coil can be calculated as

$$L = K\mu_0 n^2 \frac{A}{b} \qquad with \quad A = \pi R^2 \gg b^2 \qquad (3.1)$$

where b is the width of the n-turn coil, A is the inner area of the coil, r and R are the inner and the outer radii of the former, and K = μ/μ_0 is the relative permeability of the substance currently passing through the former nozzle. Considering the thickness of the former, K must be modified as

$$K' = K_n\left[1 - \left(\frac{r}{R}\right)^2\right] + K\left(\frac{r}{R}\right)^2 \approx K\left(\frac{r}{R}\right)^2 \qquad (3.2)$$

where K_n refers to the relative permeability of the former material. From Eqs.3.1 and 3.2 it is clear that for high accuracy of the measurement, a large number of turns, n, a thin wall for the former, and a high ratio of A/b are advantageous.

Werner and Eise (1979) and Schule et al.(1988) used this method for on-line RTD measurement. They found, experimentally, a problem with the low sensitivity. If the input quantity of iron power is too small, the tail of the RTD curve will not be accurately measured. However, if the tracer amount is too large, the flow of the polymer will be affected, and the tracer powder may agglomerate.

In the early stages of this project, efforts were made to modify this technique to increase the sensor sensitivity. This work had two aspects: a) to find a better tracer material and prepare it in the right shape; b) to develop a more efficient sensor technique.

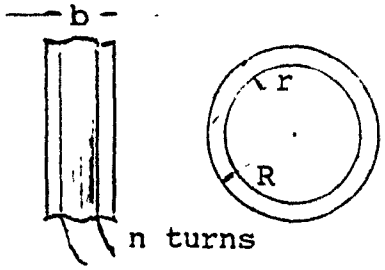

Figure 3.1 A sensor coil

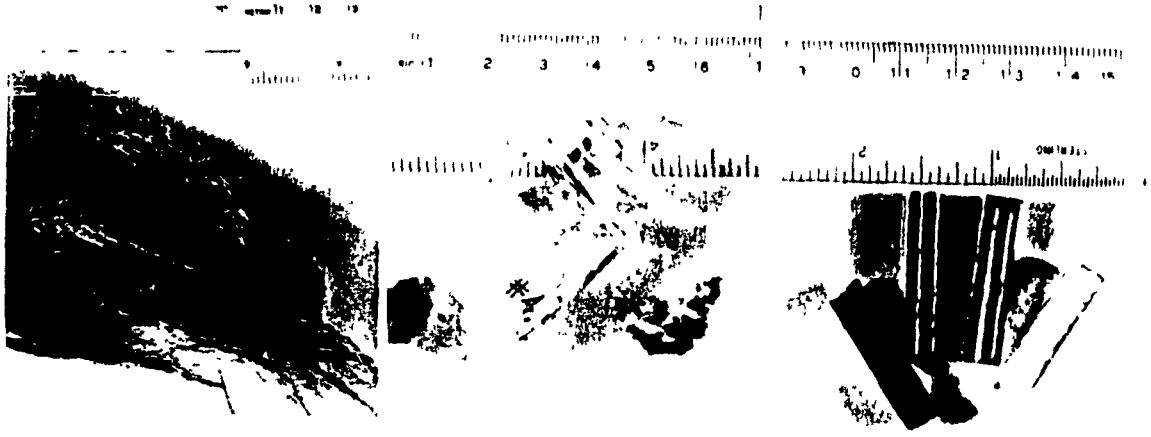

(a) Original fibres (b) Cut to powder-like (c) Samples for testing

Figure 3.2 Newly developed tracer material

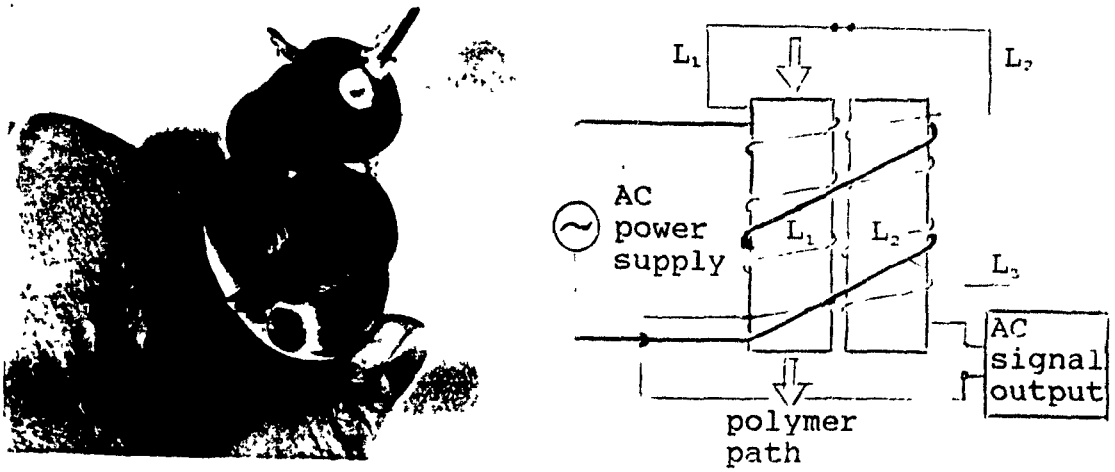

Figure 3.3 The triple-coil sensor and its diagrammatic circuit

The tracer material finally chosen was a non-crystalline, cobalt-based, ferromagnetic material newly developed in the Department of Physics of McGill university. The material was supplied in fibre form with an average length of about 150mm and a diameter of about 15μm (see Figure 3.2 a). It was reported to have a relative permeability ten times higher than pure iron and to maintain this permeability at low magnetic fields and high temperatures. For use as a tracer, the fibres were cut into lengths of about 0.1-0.3mm having a length to diameter ratio of 7 to 20 (Figure 3.2 b). Preparing the material in this shape enhances the paramagnetic effect, especially when the fibres are oriented along the magnetic field. The tracer material was mixed with epoxy resin to make samples for testing (Figure 3.2 c). The inductance changes, ΔL, were measured by inserting and removing the samples from the coil. A comparison was made between material from the Physics Department and pure nickel powders (Johnson Matthey LTD, 99.9%, -300mesh) and purified iron powder (Fisher, I-61, electrolytic powder). A factor of 52 (in ΔL) was found between our material and the Ni powder, and a factor of 22 (in ΔL) was found between our material and the Fe powder. It was noted that the material used in this test contained a lot of spherical dust and had a random orientation with respect to the coil. By purifying the tracer fibres and, as in the real case in extrusion, by orienting them along the axial direction, we could gain even more sensitivity.

A new design of a magnetic sensor structure was investigated. The sensor had three coils, L_1, L_2, and L_3 as illustrated in Figure 3.3. L_1 and L_2 were wound as two small identical solenoids put side by side and were wrapped by L_3. Coil L_3 (350 turns) is the stimulation coil linked to an AC power supply to generate an alternating magnetic field. L_1 (1000 turns) is the measuring coil with the polymer melt passing through its former nozzle. L_2, used to balance the zero, has the same structure and number of turns as L_1. A small steel screw was installed in the L_2 former nozzle for on-line fine zero adjustment.

The advantages of this new sensor structure are:

I) By putting L_1 and L_2 side by side and covered by L_3, we got better dynamic zero balancing and reduced noise.

II) By separating the excitation coil L_3 from L_1 and L_2 (different from the traditional Wheatstone bridge circuit), we get three benefits:

(a) by increasing the L_1/L_3 ratio a higher sensitivity can be gained, and a better signal/noise ratio is obtained.

(b) since the stimulating current only passes through L_3, very thin wire can be used to wind L_1 and L_2 to get more turns in a fixed space.

(c) a separate AC power supply (not from the Wheatstone bridge) can be chosen with whatever current and frequency we prefer.

The new structure provided the opportunity to adopt the

resonance technique. In the traditional L (or X_L) measurement, the stimulating AC power comes from the Wheatstone bridge or the LRC meter itself. This kind of power supply usually provides a low current and a low, fixed frequency which normally ranges from 1KHz to 10KHz, depending on the type of meter. In Schule's case (1988), for example, the frequency was 5KHz. Working at that frequency, the signal coming out of the measuring coil is very weak, and a pre-amplifier is necessary before signal processing. In the present project, the stimulating power provided to L_3 comes from a HP Model 133 Generator (sinusoid wave). Its frequency is adjusted very close to but a little bit lower than the resonance frequency of the sensor coil. Working at this frequency, the sensor gain is dramatically increased and the noise level decreased.

Figure 3.4 shows the frequency response of the sensor with the magnitude of the stimulating power fixed at three volts (1/2 peak to peak value). The upper curve was obtained by inserting into the coil former a sample containing tracer material at a concentration of 78 mg/cc. At any given working frequency, the reading from the lower curve in Figure 3.4 was the background signal which could be biased out beforehand. The difference between those two curves, at the working frequency, was the useful signal sent out by the sensor. It is clear from the plot that by working at the resonance frequency (f≈73KHz in our case), the sensor sensitivity was about 50 times higher than that at the regular frequency of 10KHz.

Furthermore, the oscilloscope showed that only when f≥60KHz did we get a perfect sinusoid output wave, while at f=10KHz the wave was seriously deformed. This means that by using the resonance technique we not only increased the sensor gain but also increased the signal/noise ratio dramatically.

By knowing the highest tracer concentration that the sensor could deal with in the on-line RTD measurement, it was easy to determine the best working frequency, which was close to but never greater than the resonance frequency. This is shown in Figure 3.5 (the higher the concentration, the lower the resonance frequency).

Figure 3.6 shows the linearity of the sensor. It covers the anticipated concentration range for the RTD measurements (corresponding to a 1-2 grams of pure tracer material per impulse injection). The stimulating power was 75.5KHz / 6V (1/2 peak to peak value).

Figure 3.7 shows that, by adjusting the stimulating power to 10 volts (1/2 peak to peak value), the new sensor had a very high output signal level that was sufficient for direct signal processing (AC signal). The same tracer sample was used for this test as was used in Figure 3.4.

As reported above, by adopting a new ferromagnetic material and introducing the resonance technique, my contribution to this method is the lifting of the sensitivity by a factor of 1000 (22x50=1100). I thus made this method more effective in competition with other methods used for on-line RTD measurement.

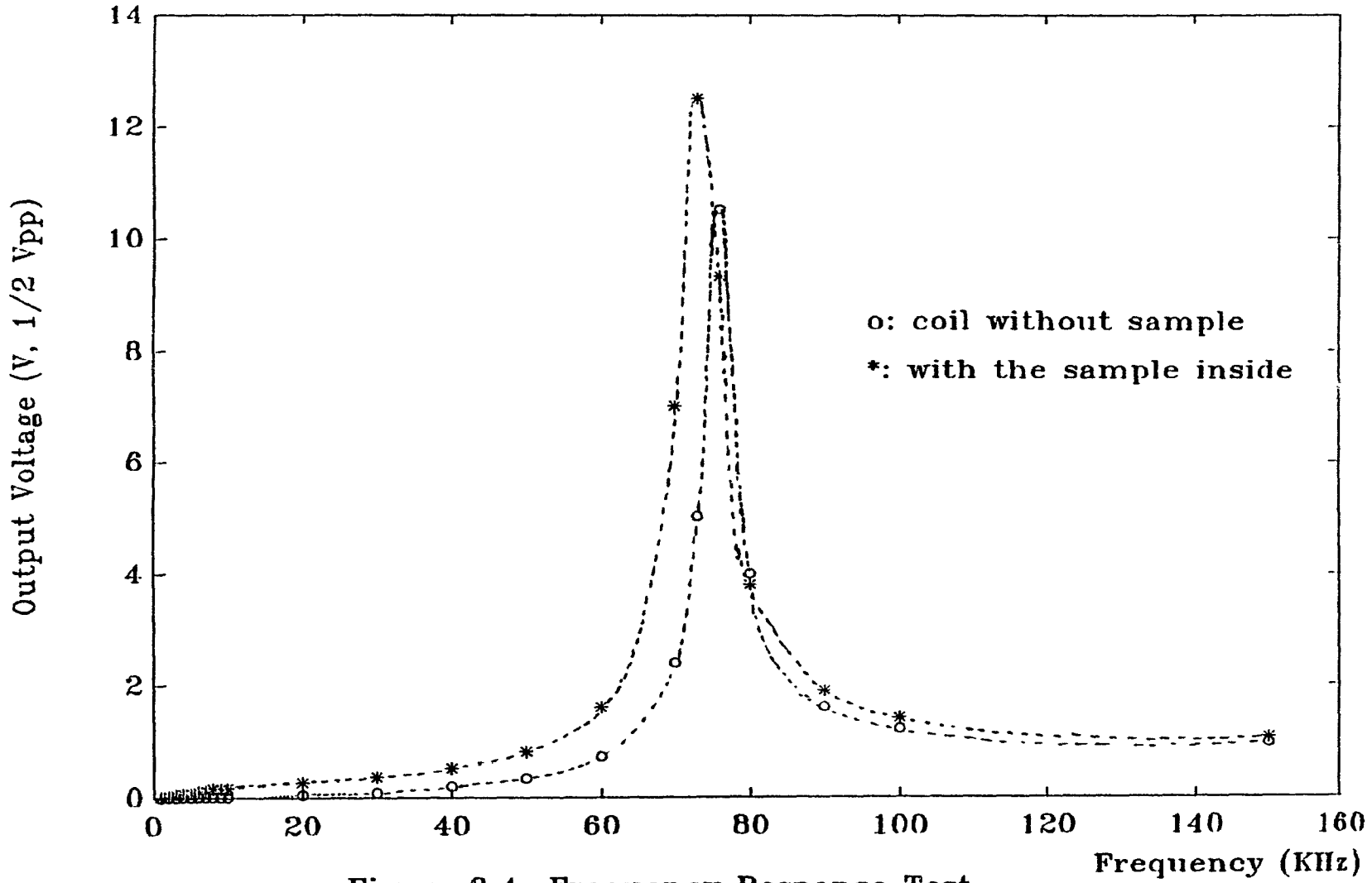

Figure 3.4 Frequency Response Test

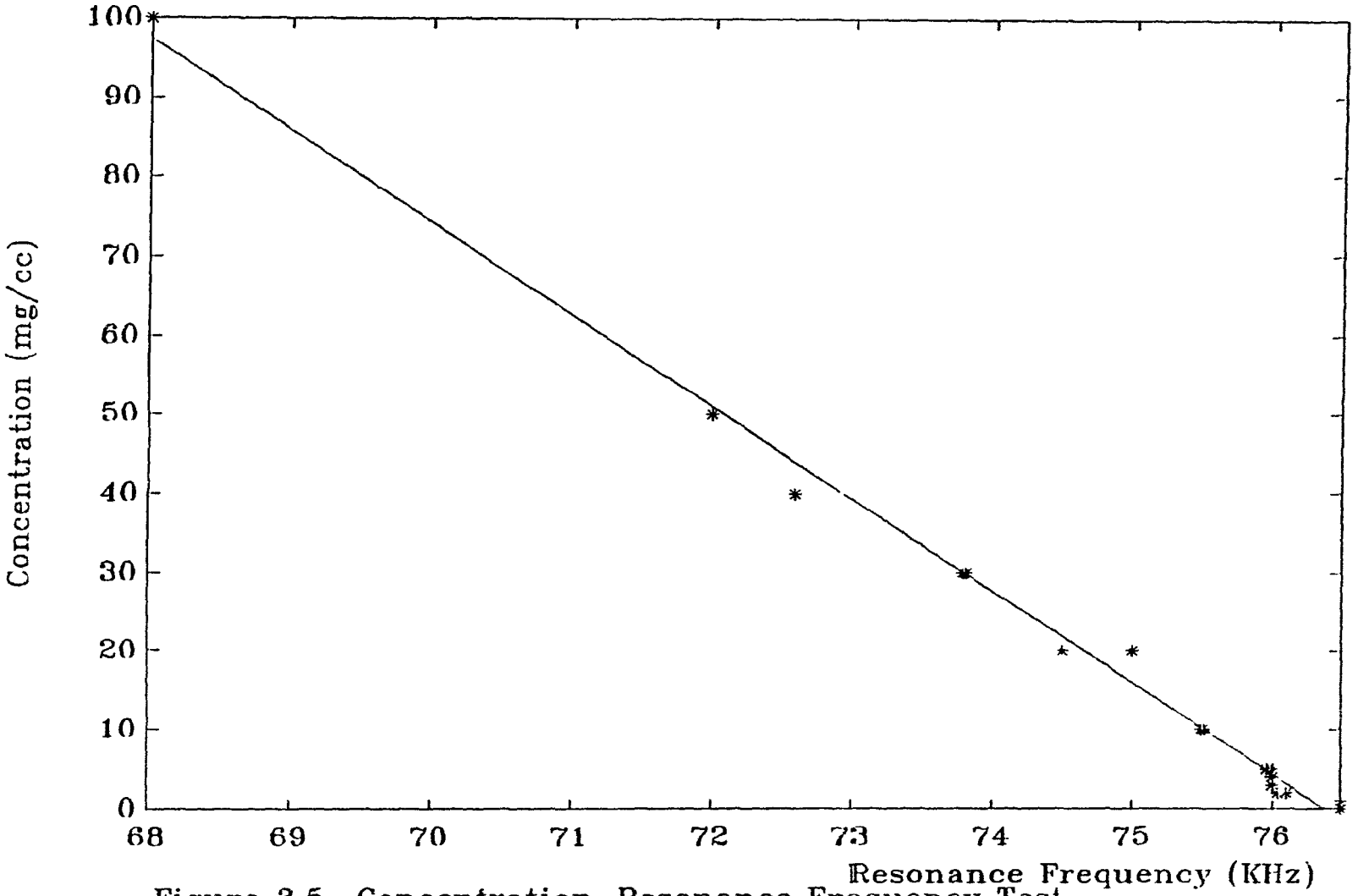

Figure 3.5 Concentration–Resonance Frequency Test

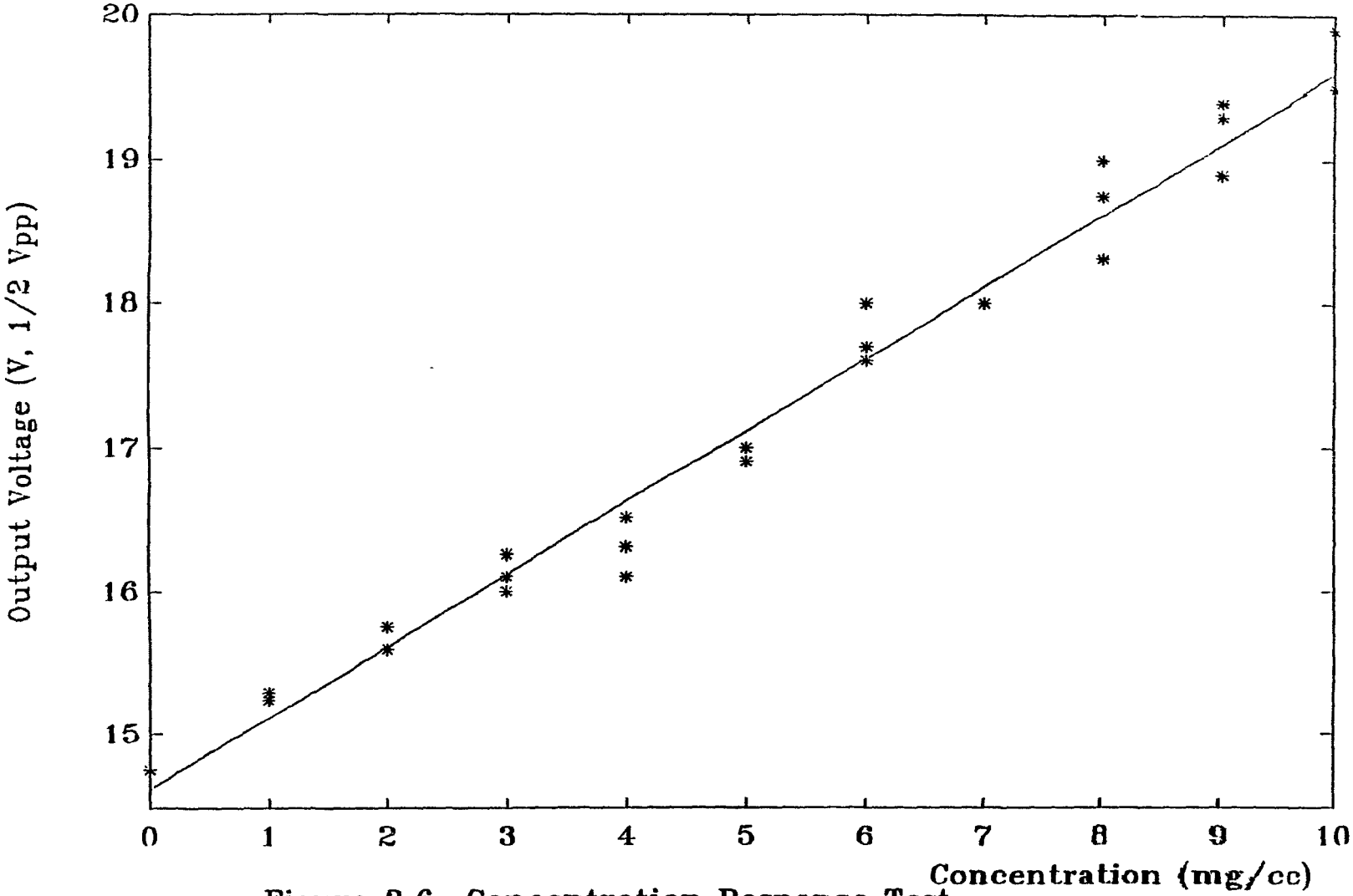

Figure 3.6 Concentration Response Test

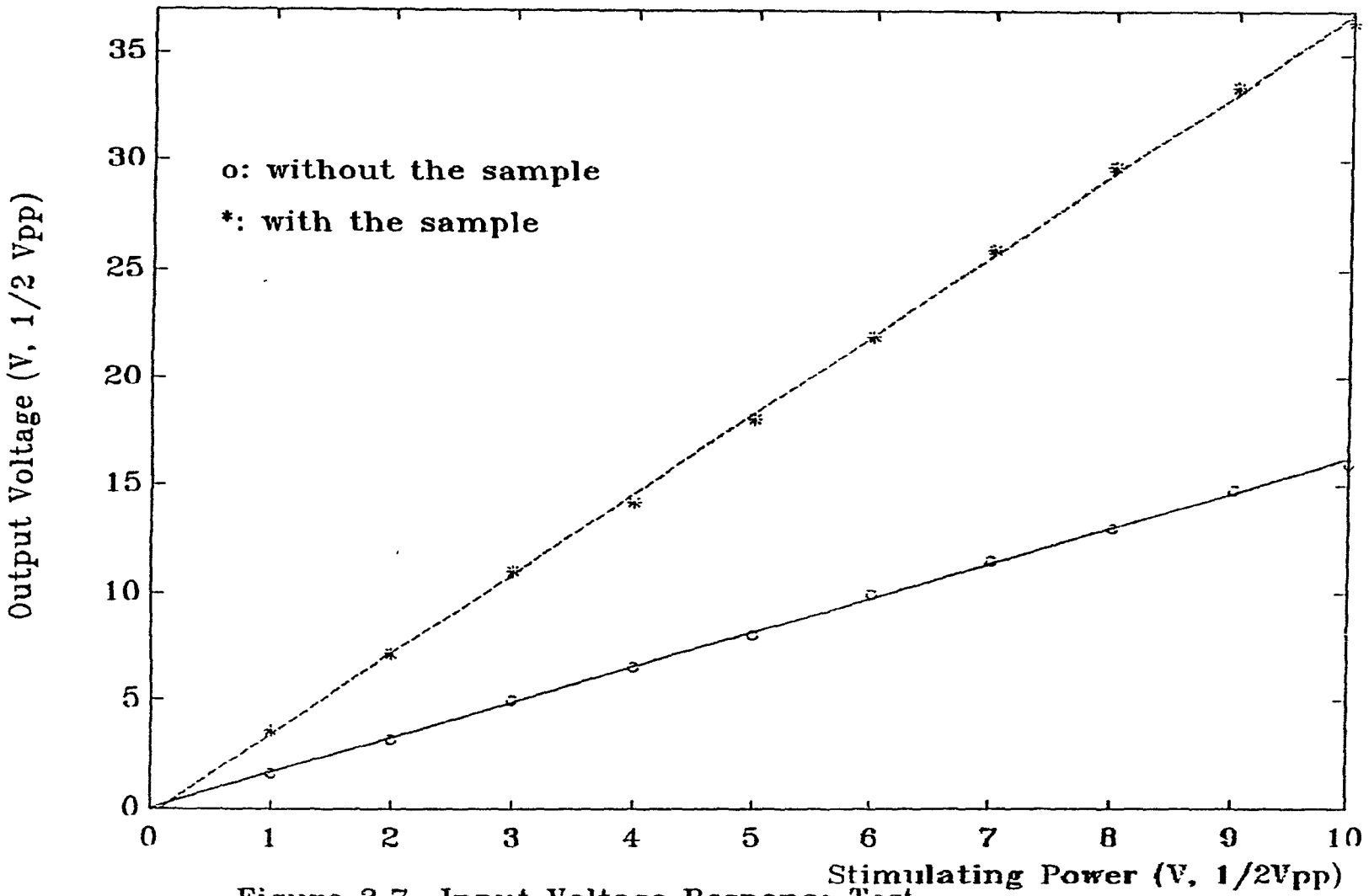

Figure 3.7 Input Voltage Response Test

3.3 Optical Methods

Besides radioactive or magnetic tracers, dyes or pigments are often chosen as tracers, since most molten polymers are transparent in their unpigmented state. There are a variety of dyes and pigments available for optical RTD measurements, and many of these are inexpensive. Following tracer injection, extrudate samples are collected and marked in time sequence. Then the tracer is leached from the sample or the whole sample is dissolved to make a dilute solution. A colorimetric transmittance test is then performed for each solution to determine its tracer concentration. The use of dyes and pigments also makes possible the visual monitoring of the test while it is in progress. The disadvantages of this method arise from the requirement of more complex equipment for colorimetric analysis and the non-linearity of colour absorption with concentration, which reduces the accuracy of the measurement.

Early usage of this method dates from 1974 when Bigg and Middleman (1) used a red food dye in aqueous solution and measured the tracer concentrations in the extrudate samples by means of a spectrometer. Kemblowski and Sek (1981) measured the pigment concentration microscopically. Kao and Allison (1984) and Cassagnau et al.(1991) used UV spectrometers. Bounie (1988) used both an atomic absorption spectrophotometer (to detect zinc oxide) and a colorimeter (to detect erythrosine). All of these are off-line measurements since sophisti-

cated instruments with special light sources are required making it difficult to do on-line.

It was only recently that successful on-line optical RTD measurements were made. Potente and Schultheis (1989) made their on-line RTD study using an optical technique, but no details were reported. In 1990, Bur et al.(4) reported on-line RTD measurement using a fluorescence spectroscopy method. They used an argon ion laser beam as the light source and coupled the fluorescence signal through an optical fibre probe to the detector.

A new optical on-line RTD measurement technique was developed for this work using a He-Ne laser as the light source, and the transmittancy of the polymer at the extruder outlet was monitored by a photomultiplier. A cell was designed to channel the polymer flow. Details of this method as well as the results are presented in the following chapters.

3.4 Summary of Method Choice

Previous sections discussed three major methods used in RTD measurement. In this section we make a brief comparison between them and explain the final choice.

The radiological analysis method has the highest sensitivity. However, the use of this technique is limited by the extraordinary precautions required to handle radioactive species, the availability of nuclear reactor facilities, and the non-trivial calibration and analysis procedures required

to generate distribution curves. Our laboratory conditions precluded this method.

The magnetic method is simple and safe but has a low sensitivity. The rheological interference caused by the necessary ferromagnetic tracer concentrations limits its usage to use with high viscosity melts. It is worth trying though in our case since we deal with polypropylene. Efforts were made early in this project to increase the sensitivity of this method, but the method was abandoned since sufficient tracer material in the proper form was not available.

We finally chose an optical method using a laser beam as the light source and monitoring the transmittance by a photomultiplier, since there is no radioactivity problem to deal with, no sophisticated equipment is required, and it is easy to find a suitable tracer for this method.

CHAPTER 4 EXPERIMENTAL TECHNIQUES

After the optical system was installed and calibrated, several groups of experiments were run on a ZSK-30 extruder using polypropylene (PP) as the working polymer. The tracer was 1 weight percent carbon black in PP, introduced by hand into the extruder through the hopper almost instantaneously. The concentration of carbon in the extrudate was monitored by the laser-photomultiplier system, and the output signal was sampled by a PC computer at a frequency of 20 samples per second. Ten samples were averaged to get an effective sample rate of two per second. The apparatus and corresponding techniques are described in following sections.

4.1 Experimental Apparatus

A schematic view of the experimental apparatus is shown in Figure 4.1. There are three major components: the extruder, the absorbance measurement instrumentation, and the data

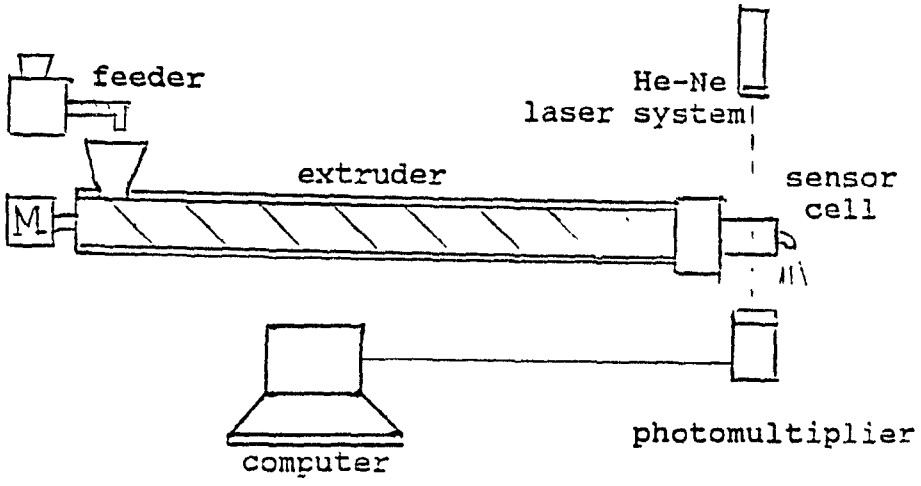

Figure 4.1 A schematic view of the experimental set-up

acquisition system.

4.1.1 The Extruder

Experiments were carried out on a Werner & Pfleiderer ZSK-30 co-rotating, intermeshing, twin-screw extruder. The modular screws were designed to be suitable for reaction extrusion. Most of the screw elements are double-flighted conveying elements with a positive pitch. The diameter of the screw is 30.7mm, and the effective screw length is 880mm. There are four zones, as shown in Figure.4.2. The feeding/melting and reaction zones are separated by two negative-pitch kneading elements. A single-flight, negative-pitch screw element is used to seal and separate the reaction zone from the devolatilization zone. There is no inherent separation between the devolatilization zone and the pumping zone.

The barrel temperature is controlled in four independent zones by a MACO-8000 control system. This system also controls the motor and the feeder.

The feeder is a K-Tron model HO DDSR 20-10 loss-in-weight two-screw feeder equipped with a Brabander controller. The control action has a 5-second period. The accuracy was tested by weighing the half-hour cumulative feed amount and comparing this with the value calculated from the feed rate set point. A rather small error, less than ±1.5 percent was found, but the instantaneous feed-rate fluctuation was occasionally as high as 15 percent. This might cause some error on the measurement.

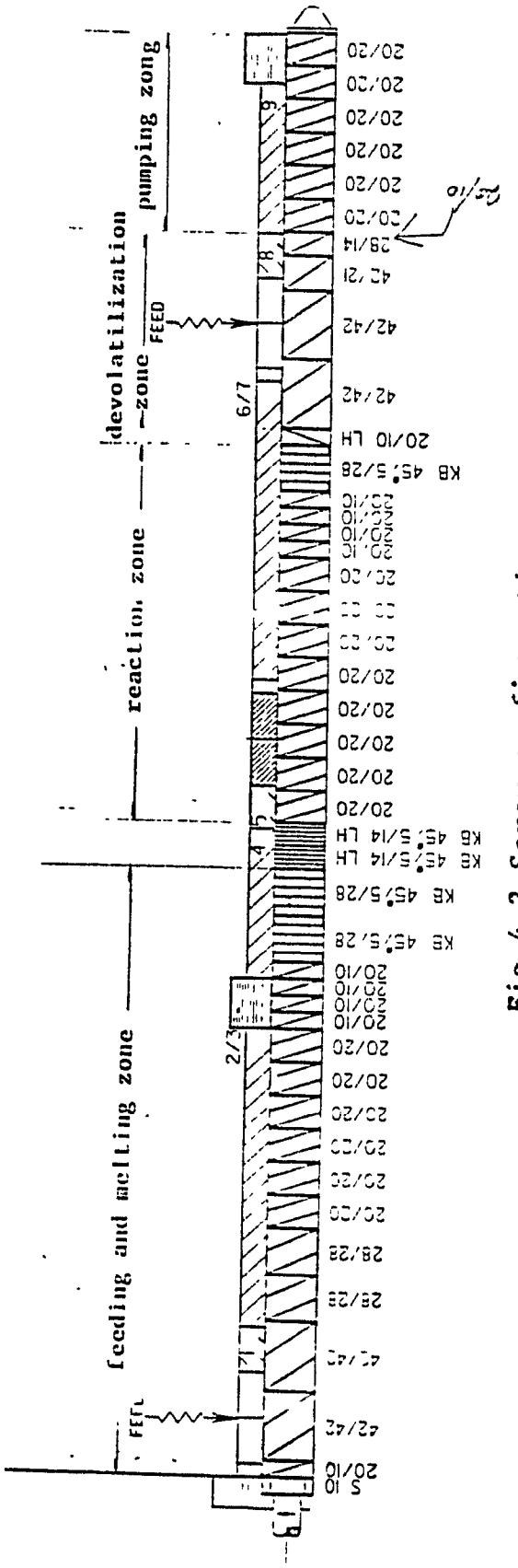

Fig. 4.2 Screw configuration
(From Werner & Pfleiderer Co.)

4.1.2 The Light Absorbtion Measurement

This system consisted of an OPTIKON LM-5 He-Ne laser source, an ORIEL Model 7070 photomultiplier detection system, and a quartz window cell. The laser and the photomultiplier were mounted on an independently mounted optical bench that was well aligned in the vertical direction. This isolated it from the mechanical vibrations generated by the extruder. The He-Ne laser emitted a monochromic light at a wavelength of 633nm. The beam shown vertically downwards passing through the cell containing the extrudate. Part of the light was absorbed to an extent corresponding to the concentration of carbon black in the polymer. The flux of the transmitted light was detected by the photomultiplier to determine the tracer concentration in the extrudate.

The laser beam, after passing through a x15 expander, had a diameter of about 14mm. To ensure uniformity of the light intensity, only the central part was used, with a diameter less then 12mm.

The sensor cell consists of a base and a cover, shown in Figure 4.3, each having a quartz window 12mm in diameter. The extrudate enters from the right through the connecting pipe, passes through the inner channel defined by two inserts, and exits through the left pipe. The whole cell was covered with thermal-insulation material leaving only the window exposed. Two 50w/220v cartridge heaters and a J-type thermocouple are embedded to control, via the MACO-8000 system, the cell temperature.

I. the cover

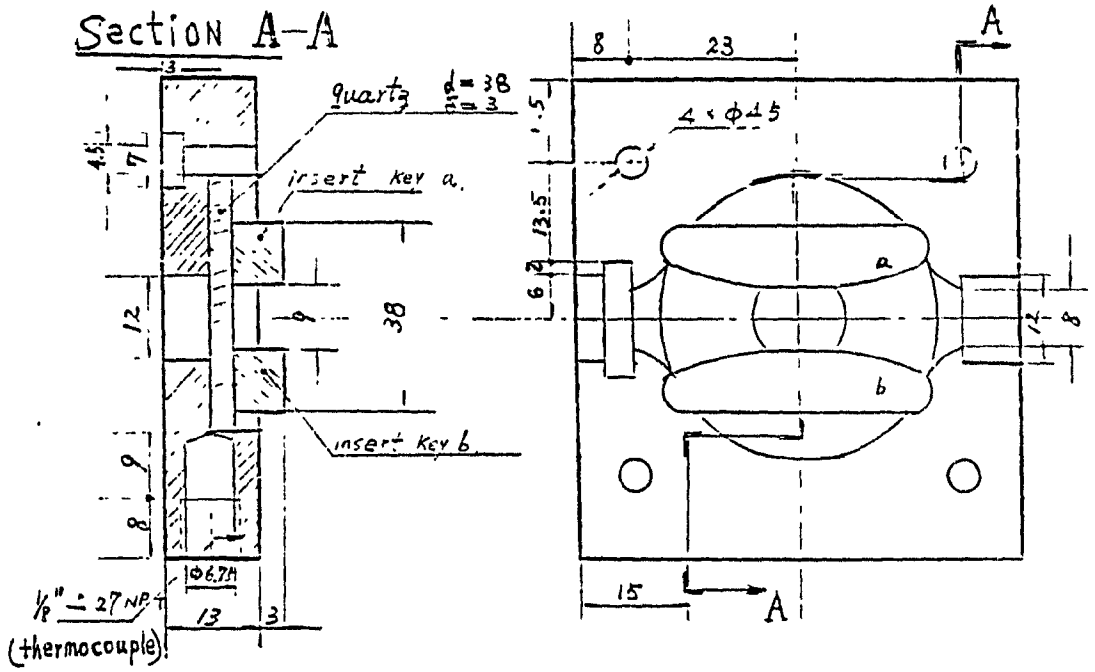

II. the base

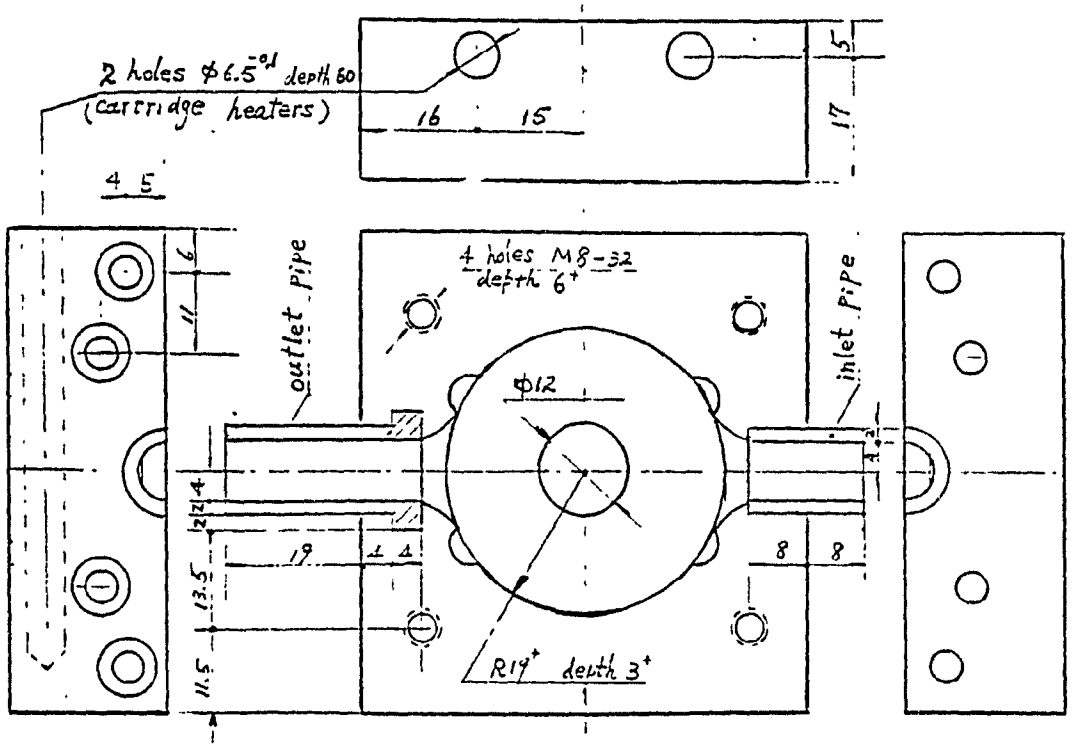

Figure 4.3 The sensor cell structure (scale 1:1, units in mm.)

An optical filter was used with its pass band centred at 633nm. The filter was positioned just above the photomultiplier, and the gap between them was surrounded with a tube of black opaque paper to exclude ambient light. The absorption measurement, by nature, does not require a single wavelength light source. The role of the filter is to prevent the ambient light from disturbing the photomultiplier, since an opening between the laser expander and the sensor cell is unavoidable, but only a very very small portion of the background light has a wavelength of 633nm. Comparative tests showed that most of the ambient light disturbances were filtered out in this way.

4.1.3 Data Acquisition System

The experimental data were acquired by an IBM-PC compatible computer via a data I/O DT-2801-A interface board. The board accepts an analog signal from the photomultiplier system probe, digitizes it and then stores it directly into computer memory. Several software selectable input voltage ranges are available. The appropriate range is selected by the data acquisition program (written in QuickBASIC, see Appendix 2.) to give the best possible signal resolution.

4.2 Tracer Technique

In optical methods, carbon black (black) and titanium oxide (white) are often chosen as tracer pigments, since they have a very small particle size, a strong optical response over a broad wavelength range, and are not expensive. The most

successful tracer formulation technique is to load the base polymer (PP, in this case) with the pigment by melting and mixing them. The pigmented polymer with, typically, 1% to 5% by weight of pigment is the tracer (40). Both carbon black and titanium oxide were evaluated following the method described above. It was found from the concentration-absorption test of the tracer samples that the titanium oxide samples had poor dispersion and were non-uniform . Furthermore, during the mixing procedure, some unknown reaction occurred, which generated some black colour. This appeared to be polymer degradation. It may have been caused by a trace amount of copper or the cleaning compound used to clean the mixer between batches. For that reason, we finally chose carbon black as the only tracer for our RTD measurements.

4.2.1 Tracer Preparation

Three tracer materials were prepared for the RTD measurements, with concentrations of 1%, 2%, and 5% by weight. Two batches of tracer having lower concentrations were also prepared in order to accomplish the on-line sensor calibration.

Three steps were taken in the preparation procedure to ensure the concentration uniformity (statistical) of the tracer material. First, certain amounts of carbon black and PP were melted and mixed in a Brabander blender. The blender has a capacity of about 50cc, and 40 grams of marked polymer were made in each run. The PP was charged first, blended and heated

until melted, and then the carbon black powder was added gradually with the blender running to avoid agglomeration and the stick-on-the-wall problem. Each batch was cut into 3 to 5 pieces, and all the pieces from different batches of the same concentration were mixed together. In the second step, 2 or 3 pieces were randomly chosen, heated and pressed into a thin sheet about 240mm in diameter and 0.3mm in thickness. Finally, these sheets were cut into small pieces with an average size of 1 x 1 x 0.3 mm. A large number of these tiny pieces were thoroughly mixed to produce the tracer material.

Part of this tracer material was used to make the lower concentration tracers (0.01 mol and 0.04 mol) prepared for the sensor on-line calibration. The mixing was done in a 1kg capacity Banbury mixer. The mixtures from different batches were cut and ground into small pieces with dimensions of 3 to 5mm.

4.2.2 Injection Technique

The injection of the tracer should ideally be accomplished with a minimum upset to the system over a period of time that is very short compared to the mean residence time of the extruder.

To ensure fast injection, ordinary 5cc plastic syringes were modified. The end of the syringe barrel was removed so that, at the end of an injection, the plunger came out of the barrel. An anti-static liquid cleaner was used to prevent the tracer particles from sticking to the syringe barrel wall. The

inner and the outer surfaces of the syringe barrel were treated with unit-static cleaner just before filling it with tracer. The syringes were then used for injections the same day, before the anti-static treatment lost its effectiveness. It was estimated that an injection could be thus accomplished within 0.1 second. Compared to the mean residence time of the extruder, which is in the order of 50 seconds, this is an excellent approximation to an impulse.

In order to generate an instant plug flow, the amount of tracer in one injection should fit roughly in the open chamber of the extruder screws under the hopper. The amount we used in our experiments was 0.2 to 1 gram. Various methods for avoiding a disturbance to the feed rate, caused by the injection of the tracer material, have been used in the past. Janssen (1979) temporarily stopped the feeder, while Todd (1975) used a 4-way valve. Janssen's method was not applicable in this work, since the response time of the feeder was several seconds. Todd's approach was judged to be overly complex. The problem was solved in this work by diverting the feed manually during the injection. This simple method is fast and reliable and, with practice, the exact amount was diverted.

The effectiveness of the injection technique and tracer preparation method were demonstrated by the reproducibility of the experimental data.

4.2.3 Detector Calibration

All the instruments composing the detector system were carefully calibrated beforehand, and an overall tracer concentration/response signal on-line calibration was carried out for the whole detector system, in order to guarantee an accurate measurement.

The off-line calibration of the instruments included:

i) verification of uniformity and stability of the laser beam,

ii) verification of linearity of the photomultiplier system and range and linearity of the computer interface board, and debugging of the data acquisition program.

Some hardware problems were solved during the calibration procedure by adding an RC filter to eliminate the noise of the photomultiplier amplifier and bypassing the attenuation circuit to get the desired signal level. But some of the problems were too complex to be solved within the scope of this project. The photomultiplier system drifting problem for example, was solved by introducing some compensating techniques in the later data treatment procedure as described in Section **4.5**.

The calibration to relate the tracer concentration to the response signal was carried out by introducing the tracer at a known concentration, C, into the extruder and recording the corresponding signal change (voltage). These changes were accomplished by using two feeders, one with pure PP and the

other containing low concentration tracer (see **4.2.1**). The PP flow rate was first set at a value, Q_1. After steady state was achieved, a command from the computer changed its set-point to Q_2 and set the other feeder to a flow rate q such that $q+Q_2=Q_1$. The tracer concentration C was thus:

$$C = C_0\left(\frac{q}{q+Q_2}\right) \qquad (4.1)$$

where C_0 is the concentration of the originally prepared tracer. A typical response is shown in Figure.4.4.

The steady state values of the step-change responses were used to form the calibration curve, as shown in Figure 4.5. Unfortunately, these calibration experiments were not repeated, since all the low concentration tracer material was used up.

A conservative tracer concentration range was used in the RTD measurements. The maximum concentration at the peak of the RTD curves never exceeded 0.07 g(C)/kg(PP).

4.3 Experimental Procedure

It was found that the alignment of the optical system plays an important role in our experiments. It was not enough to ensure that the laser beam, the cell window, and the photomultiplier were on a common axis. There was always an angle of several degrees between the normal to the cell window and the laser beam. This angle affected the reflection of the laser beam, and variations in the reflection destroyed the

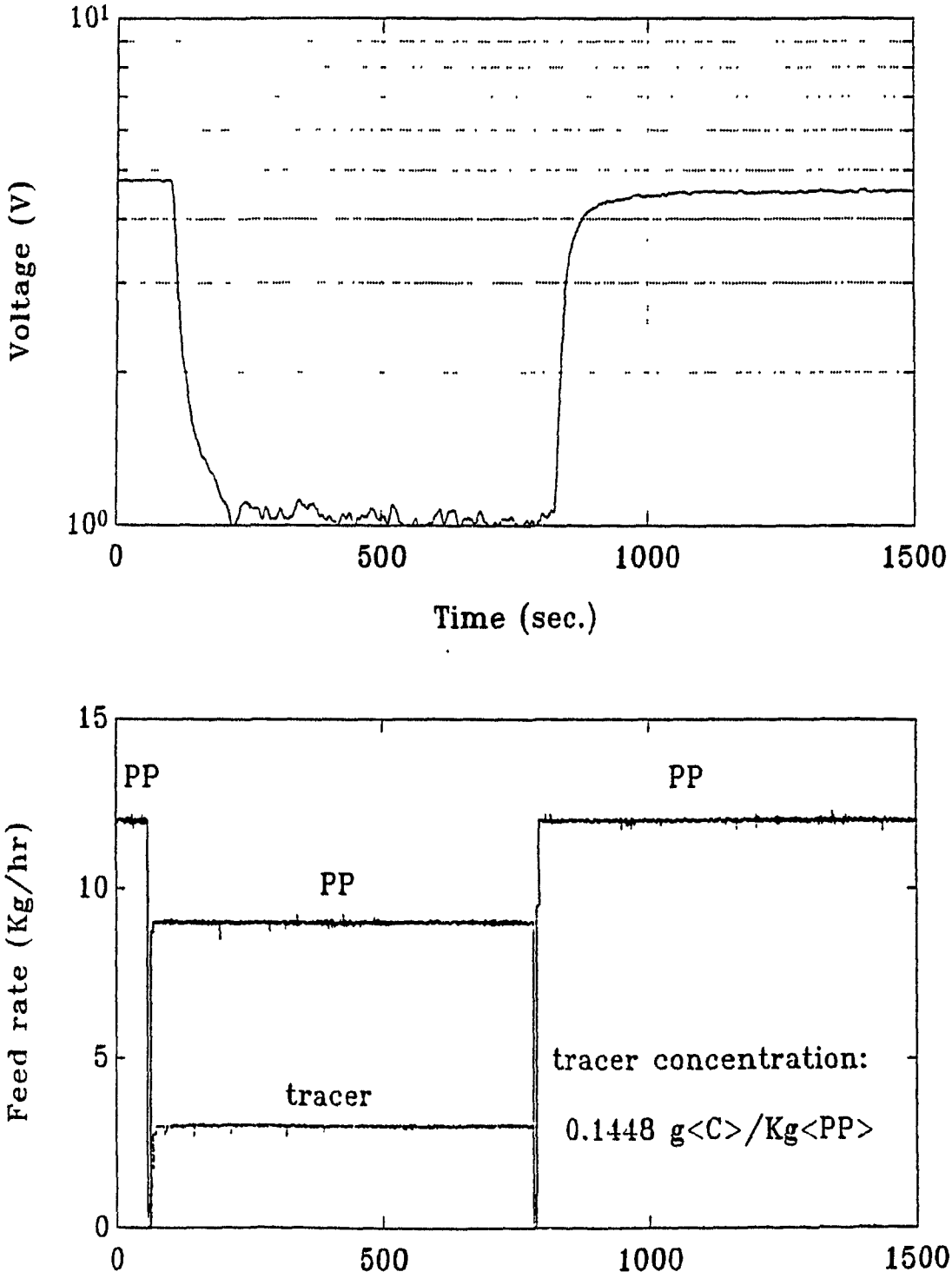

Figure 4.4 A step change response

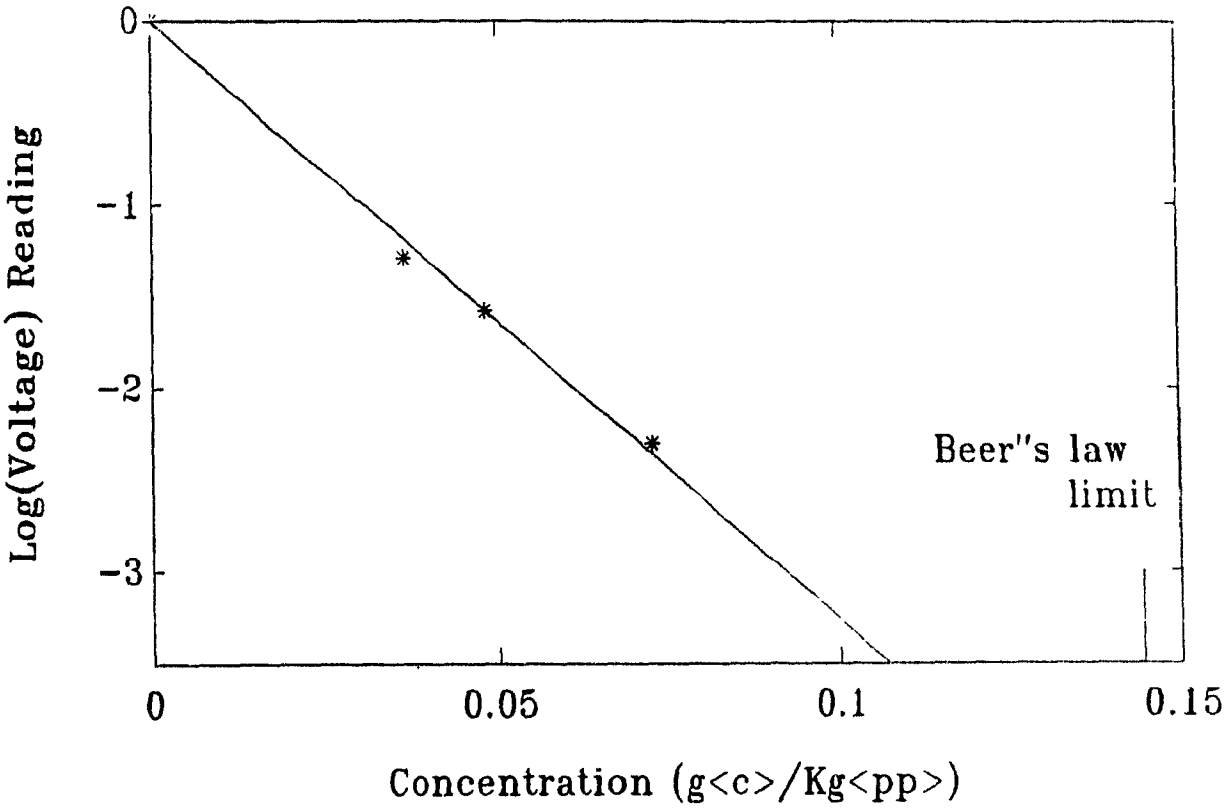

Figure 4.5 Sensor system calibration

reproducibility of the experiments. The best alignment procedure was to proceed from top to bottom, i.e., to adjust the laser tube position first, and then the photomultiplier. The position and direction of the laser tube (with the expander) should be so adjusted that the laser beam completely covers the cell window, and the spot reflected from the window is at the centre of the expander lens. This ensures that the laser beam is perpendicular to the cell window. Similarly, the position and orientation of the photomultiplier were adjusted to let the light spot fall on the centre of its lens, and it was ensured that the window shape was shadowed correctly on the photomultiplier. After the optical system was aligned, it

was not touched again during the experiments.

The electronic instruments were adjusted by the following procedure. First, the photomultiplier system was allowed 15 minutes to warm up after turning on the power. Then, the meter zero and the photomultiplier zero (the dark current) were adjusted carefully. Then the extruder was turned on and pure polymer was fed at the desired flow rate. After several minutes, a stable reading was obtained from the photomultiplier system output. This was the "base line" (for the RTD curve) and should be adjusted to a maximum voltage reading. The base line adjustment was accomplished by adjusting the high voltage power supply of the photomultiplier. After such adjustment, it took at least 5 minutes for the photomultiplier to reach a new steady state.

After both the sensor system and the extruder achieved steady state, I started to run the data acquisition program to count the time and to record the voltage reading for a certain preset period. The tracer was injected one or two minutes after the program was started. This was because a short segment of the base line before injection was needed to check the system condition and to perform the base line drift compensation.

Between experimental runs, the throat of the hopper was cleaned and the base line readjusted, if necessary.

To continue to the next run, the new operating conditions were set from the MACO-8000 control screen, and I waited for

the extruder to reach the new steady state. At the same time, the computer was doing the data treatment for the previous experiment and saving the 2Hz raw data onto the hard disk.

4.4 Experiment Design

To study the effects of operating conditions on the RTD, two groups of experiments were designed: (1) Feed rate trend experiments: varying the feed rate (throughput) from 4kg/hr to 12kg/hr (five value points) with the screw speed fixed at 300rpm. (2) Screw speed trend experiments: varying the screw speed from 100rpm to 300rpm (five value points) with the feed rate fixed at 6kg/hr.

Another group of feed rate trend experiments were designed with the on-line rheometer installed. Comparison of these two feed rate trends (carried out under exactly the same operating conditions) reveals the effect of the in-line rheometer on the residence time of the whole system.

The effect of viscosity on the RTD was examined by changing the extrusion temperature and by using a different grade of PP.

4.5 Data Acquisition and Treatment

Data acquisition was accomplished using a PC compatible computer and a DT-2801-A interface board. The photomultiplier's signal was sampled at a frequency of 20Hz and stored in memory. During the period that the extruder was stabilising

for the next run, a program averaged the data and saved the resulting 2Hz samples onto the hard disk. This simple averaging method was sufficient to remove high frequency noise, and no further filtering was necessary.

The RTD curve was obtained by calculation:

$$f(t_i) = \frac{C_{out}(t_i)}{\sum_0^{\infty} C_{out}(t_i)\,T} \qquad (2.18)$$

where the sample period, T, was 0.5s, and $C_{out}(t_i)$ was calculated from the recorded raw data:

$$C_{out}(t_i) = \left[\log\frac{V(t_i)}{V_0}\right] / S \qquad (4.2)$$

where $V(t_i)$ is the recorded data, V_0 is the average of the beginning section of the $V(t_i)$ curve, recognized as the "base line", and S is the slope of the V/C calibration curve in Figure 4.5. V_0 should be constant, but due to an ambient temperature change, there was always some drift. Although this drift, in terms of $C_{out}(t_i)$, was small (approximately 1% of the peak value), it affected the mean residence time dramatically, since the later part of the curve was weighted more heavily (see example in next chapter). Fortunately the drift was slow and did not change direction during a given experimental run. Thus, a base line drift compensation technique similar to that used in chromatography could be used. The start and end points of the real base line were decided from the raw data. These two points were then linked with a straight line to form the

real base line. All the $C_{out}(t_i)$ values calculated from the raw data must have this base line subtracted to get the compensated value. These compensated values were then used for the RTD and mean residence time calculations. Results are reported in the next chapter.

An example of how to determine $V_0(t)$ is illustrated in Figure 4.6, where raw data from a complete experimental run were first potted using semilog coordinates with the injection time denoted by '*'. By inspection of the curve I chose a beginning section from t=125 to 138 seconds (based on personal skill). Hence the starting point, **s**, of the base line was chosen at t=(125+138)/2=131.5 seconds, and its value was decided by averaging the data in this beginning section. Similarly the end point, **e**, was chosen at the middle of the section from t=550 to 600 seconds, and its value was the mean of the data in that section. The base line, $V_0(t)$, was then obtained by linking s and e (denoted as 'o's in Figure 4.6) with a straight line. The mean residence time thus calculated was 66.2 seconds for this set of experimental data. These same raw data are also used in the examples of section 5.1.

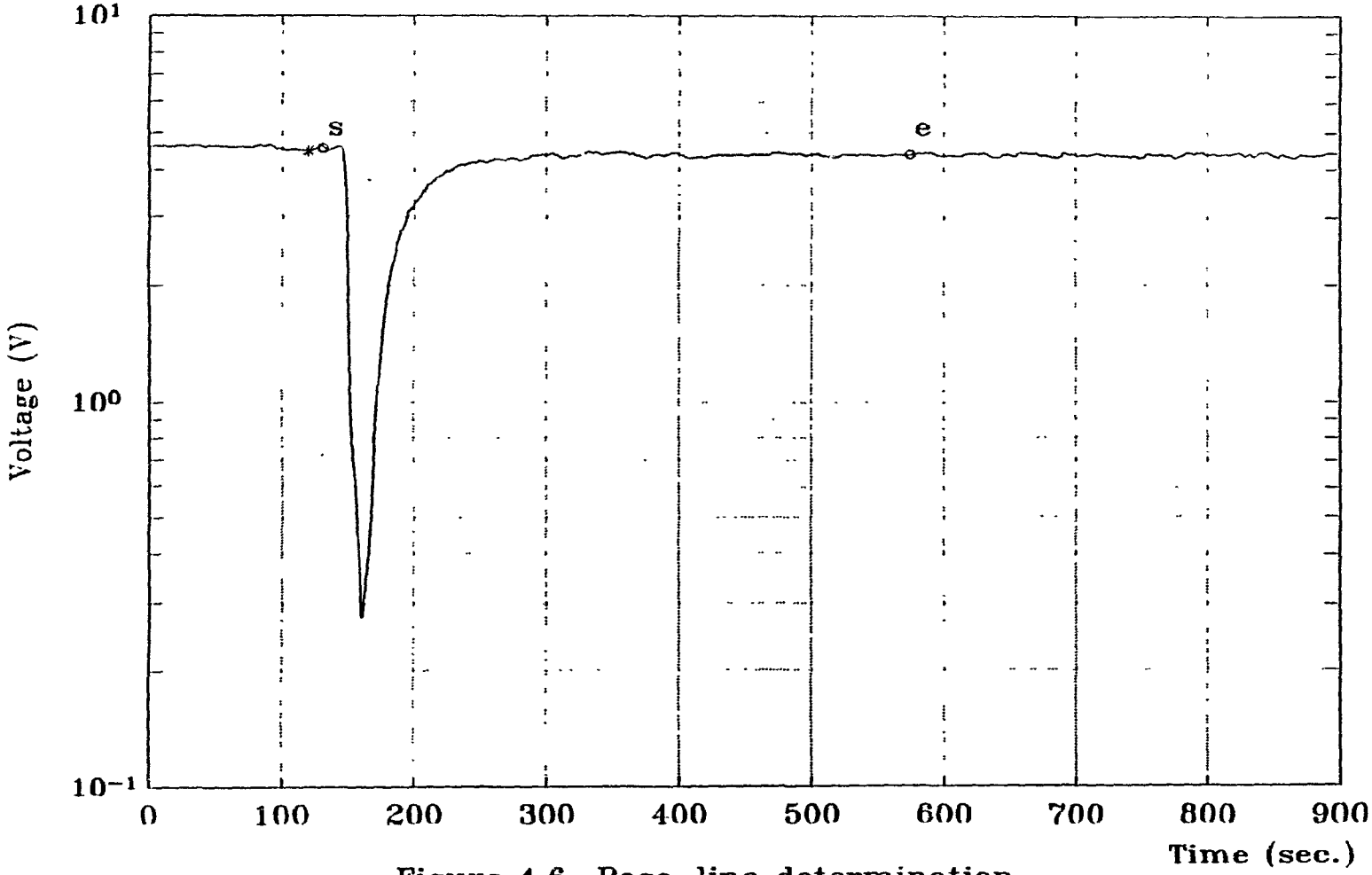

Figure 4.6 Base-line determination

CHAPTER 5 RESULTS AND DISCUSSIONS

5.1 Evaluation of the Quality of the Data

Data from a single experiment are analyzed in this section to examine the feasibility of the optical method.

5.1.1 Interpreting the Response

A typical set of impulse response experimental data (which were used in Section 4.5) is plotted in Fig.5.1 in the form of a C(t) curve. The symbol "*" denotes the time of injection of the tracer, and the residence time is counted from here. There is a short segment of horizontal line after the "*", denoting a pure delay of the response. This corresponds to the minimum residence time required for any portion of the material to pass through the extruder. The pure delay is followed by a sharp peak with a sloping tail. Most of the tracer material comes out under the peak. Generally, the sharper the peak, the worse the overall mixing and vice versa.

The RTD curve, f(t), can be obtained from the C(t) curve by simply dividing the C(t) curve by the total area under it. Value of f(t) has units of s^{-1}. To get a normalized (dimensionless) RTD curve $f_\theta(\theta)$, we first calculate the mean residence time $\bar{t}$, then multiply it by f(t) and plot the product versus the dimensionless time, $\theta \equiv t/\bar{t}$. While the C(t) curve is useful for checking the sensor response to tracer concentration, and the f(t) curve has the advantage of showing RTDs with respect to the real residence time,

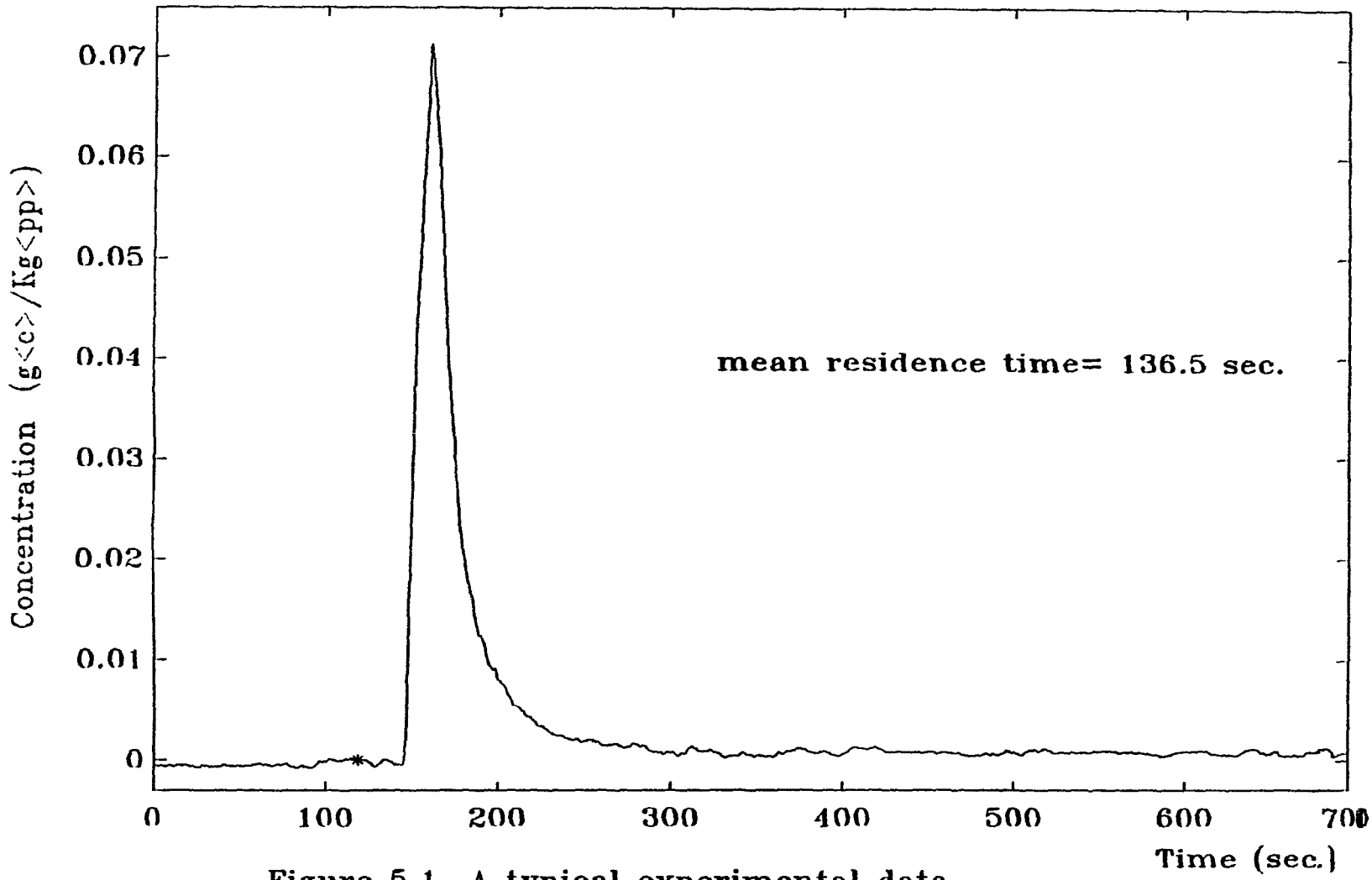

Figure 5.1 A typical experimental data

$f_\theta(\theta)$ curve is more convenient for comparing the quality of mixing (refer to **2.1.2** and **2.1.3**). All of these representations are used in the following discussion.

5.1.2 Reproducibility

The reproducibility of the experiments is an essential and critical criterion for judging the accuracy and reliability of an experimental method. The reproducibility of our experimental runs, in most cases, was very good. A typical example is shown in Fig.5.2, where the curves for two experimental runs (dotted line and solid line) at the same operating conditions are seen to be almost identical. The calculated mean residence times differ by only about 1.2% in this case.

5.1.3 Error Sources

There were several factors causing different kinds of error. Some of these were eliminated by means of more skilful operation, but some were not solved within this project because this would have required equipment modification. These latter factors are discussed below.

I). Fluctuations and drift of the photomultiplier output signal:

It was found during the off-line test of the photomultiplier system that there were periodic fluctuations with a period of about 20 seconds. These increased with an increasing output signal voltage (i.e. decreasing tracer concentration). These showed up on the RTD curve as fluctuations on the end of the tail. This is seen in the example

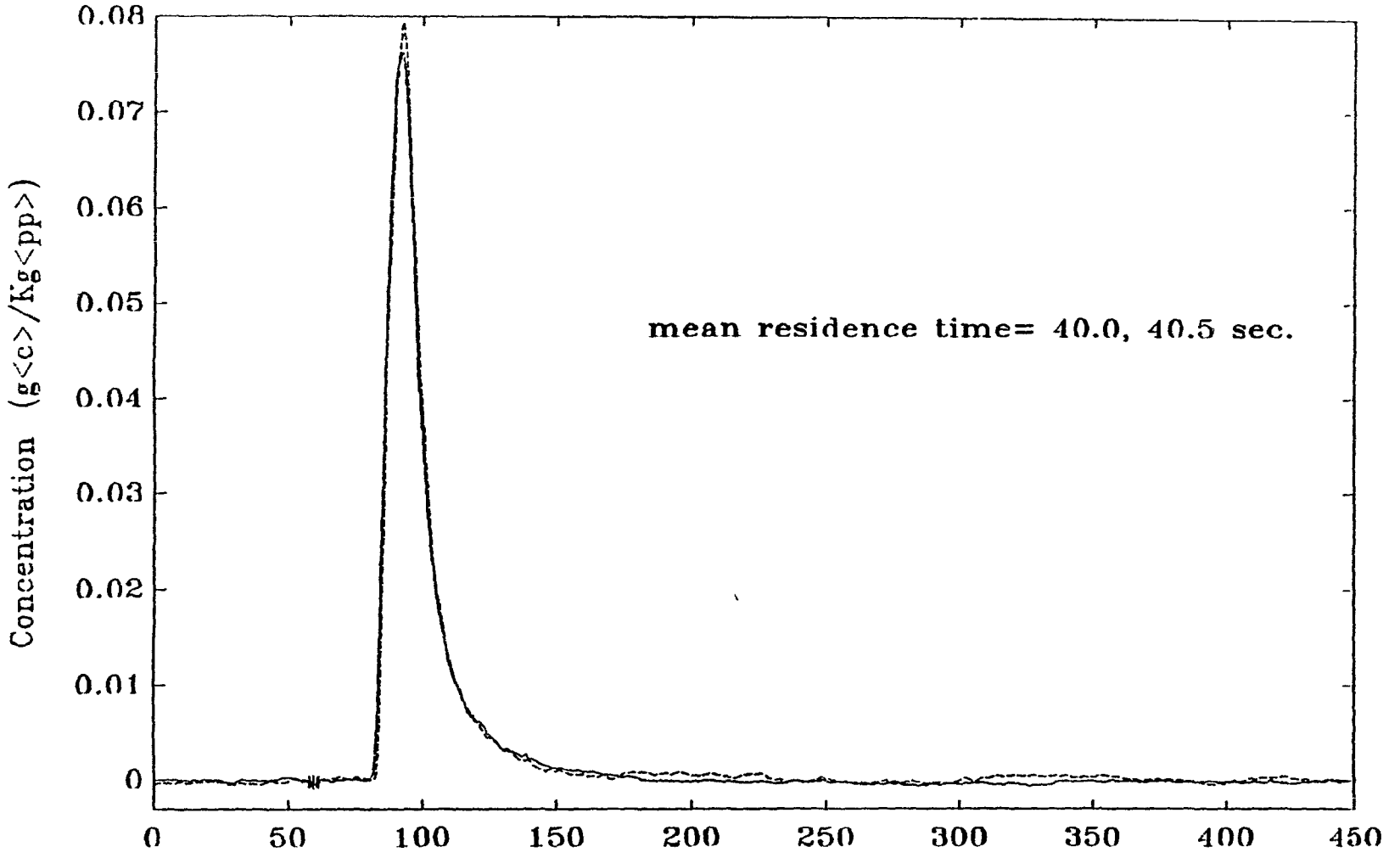

Figure 5.2 An example of reproducibility

of Fig.5.1. This kind of fluctuation had a certain magnitude. For a large peak (large amount of tracer injected) this could be ignored. But when a small amount was injected, it could cause a large error. To demonstrate this, Fig.5.3 shows the same experimental data as those in Fig.5.1 but with the tail part replaced by a straight line. The start and end parts of this straight line were established by averaging a certain section of the data. A 23.4% difference in the calculated mean residence times was found between these two Figures.

Long term drift also causes serious error. Careful examination of Fig.5.1 or Fig.5.3 shows that there was a tendency for the signal to increase in the tail zone, it never returned to its original zero. Three phenomena made us believe that this was caused by base line drift rather than a minuscule amount of tracer. Firstly this drift does not always occur, nor is it mono-directional, since negative drift was also observed. Secondly the drift depends on environmental conditions (temperature and to a lesser extent ambient brightness) but not on operating conditions such as feed rate, screw speed, barrel temperature, or the injected amount. Thirdly when certain environmental condition caused the RTD curve to drift, it also caused a drift of the pure polymer flow base line of about the same amount and same direction. This problem was treated by introducing base line compensation as discussed in Section 4.5. An example is shown in Fig.5.4, where the base line compensation corrected for a 51% error in the calculated

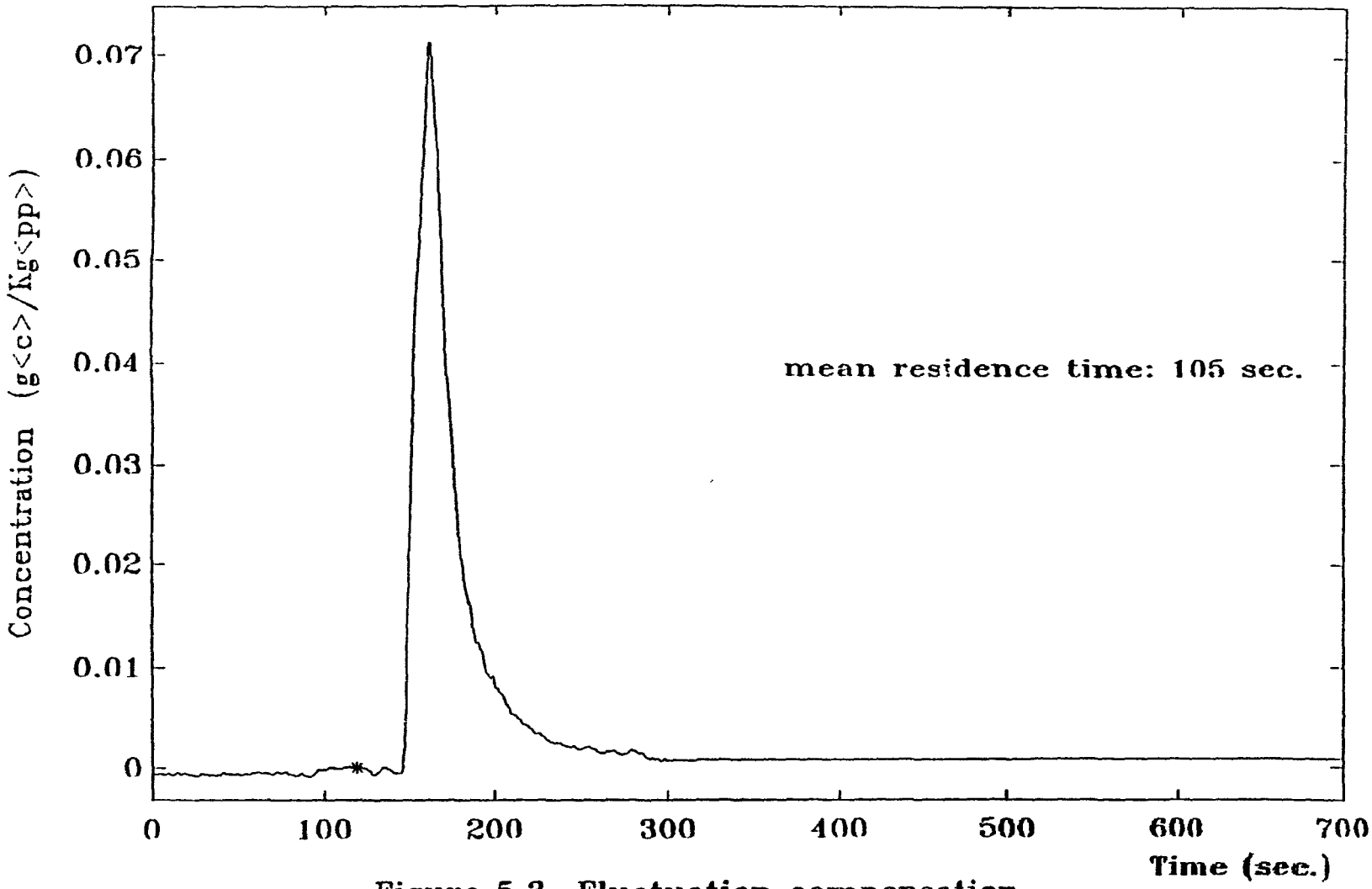

Figure 5.3 Fluctuation compensation

mean residence time. Notice that the magnitude of the drift was only about 5% of the full range voltage output or about 1.2% of the height of the concentration peak.

II). The non-uniformity problem:

The optical method of concentration measurement assumes a uniform tracer particle distribution across the cross section of the flow. However, for a twin-screw extruder, there is always some non-uniformity of the tracer concentration in the cross section of the flow at the end of the screws. Furthermore, the high viscosity of the polymer melt ensures laminar flow in the adapter section between the end of the extruder and the sensor cell and hence Taylor diffusion always occurs here. The distortion of the true RTD caused by this diffusion, and the non-uniformity of the tracer particles across the cross section, will affect the accuracy of the optical measurement. A detailed illustration of this error source is given in Appendix 1.

Careful inspection of all experimental results indicated that the main effect of this phenomenon was the deformation of the RTD curve in the neighbourhood of the peak. This may result from the fact that local saturation (concentration goes beyond the Beer's law range) exacerbates the non-uniformity problem. An especially serious case is shown in Fig.5.5. Fortunately, this part of a RTD curve is weighted lightly in the mean residence time calculation, so that the error caused by this problem was small. This problem is discussed further

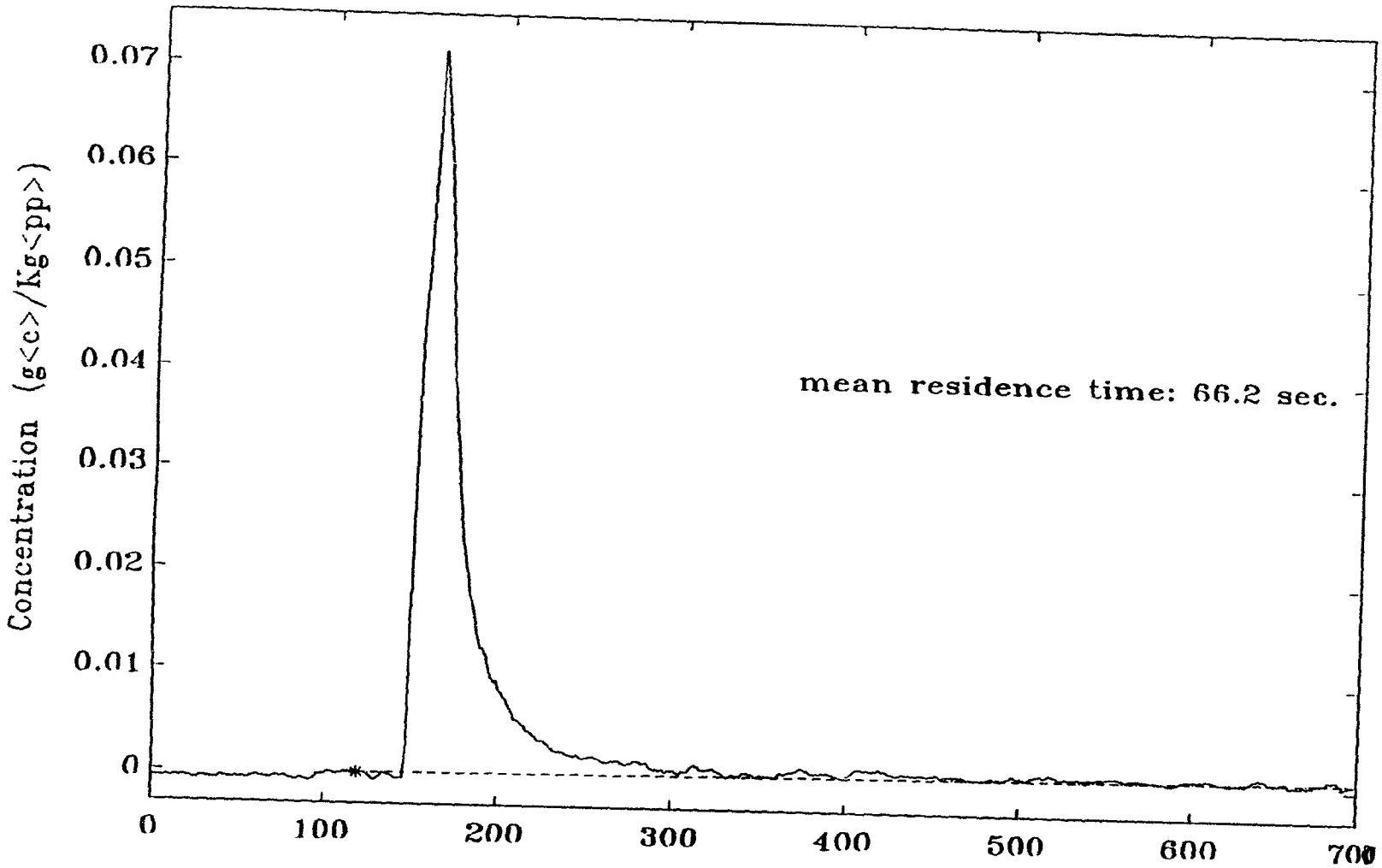

Figure 5.4 Base-line drift compensation

in next section. An attempt was made to reduce the severity of the non-uniformity effect by modifying the flow channel control key bars.

5.1.4 Over-all Mass Balance on the Tracer

Another criterion for judging the goodness of a RTD measurement technique is the over-all mass balance on the tracer. In sampling (discontinuous) experiments, sometimes it is possible to check the tracer mass balance by extracting the tracer from the total content of the apparatus after the last sample has been taken (Janssen, 1979). For example, Bounie (1988) reported a tracer recovery of 90% or more in his experiments.

For on-line (continuous) experiments one can integrate to find the total area under the RTD curve and compare this with the total amount of tracer injected. This not only verifies the recovery of all the tracer from the extruder but also requires either good linearity or careful calibration of the detector system. This method was used to evaluate our experimental results. In using this mass balance, an individual value of the integral is not important by itself since one can simply modify the sensor calibration factor to give the correct result. Rather, it is the repeatability and linearity of the tracer mass measured throughout experiments under different operating conditions that is important. In this work, it was found that varying operating conditions produces different tracer mixing pattern in the sensor cell, and this

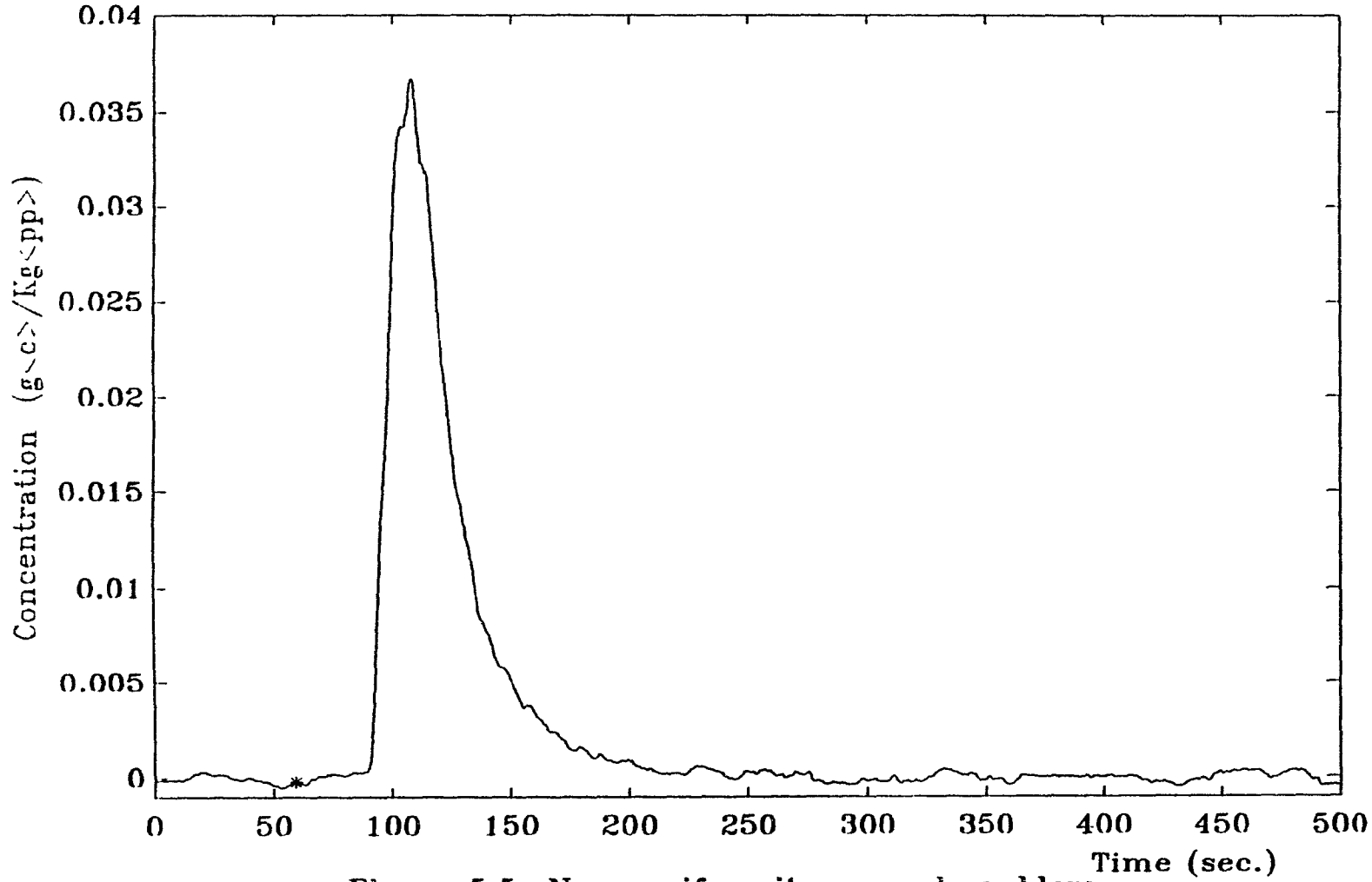

Figure 5.5 Non-uniformity caused problem

is revealed in the non-linearity of the sensor.

Several groups of experiments carried out under various conditions were checked. It was found that varying the total amount of tracer injected (converted to pure carbon black) caused the biggest variation in the mass balance calculation. Therefore we chose this divergence as one of the criteria for the accuracy/reliability of our sensor technique. A typical group of over-all tracer mass balance tests are shown in Fig.5.6, with the total injected tracer amount (pure carbon black) varying from 2.5, 5, to 10mg (cases I, II, and III in Fig.5.6).

The calculated tracer mass recoveries (in weight percent) for these three runs have a divergence of about ±12%, and the error in the mean residence time is ±4.2%. This shows that there is still room for improvement of this method. Some suggestions are given in Chapter 6.

5.2 Discussion of Results

In this section four major aspects of the experimental results are discussed, and comparisons are made with data reported in the literature.

5.2.1 The Effect of Screw Speed

Results for a set of experiments with varying screw speed, keeping other conditions fixed, are shown in Fig.5.7 in the form of normalized RTD curves. Only four of 14 experimental results are shown for clarity. The mean residence times

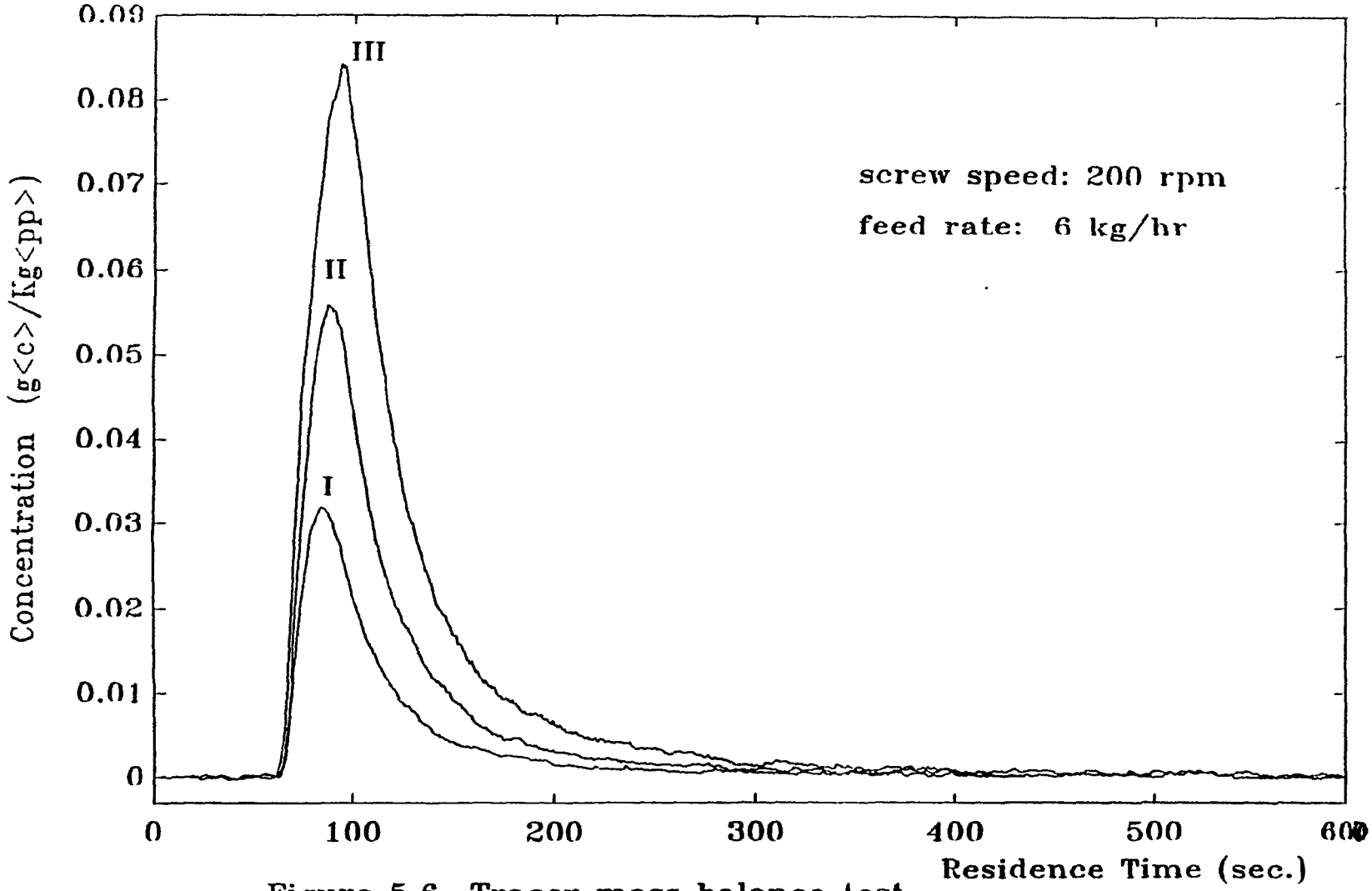

Figure 5.6 Tracer mass balance test

calculated from these RTDs are plotted in Fig.5.8. The feed rate for these experiments was 6kg/hr.

A good linear relation is indicated in Fig.5.8, with the mean residence time decreasing when screw speed increases. Presumably, this is because an increase in screw speed decreases the degree of fill. Therefore, so long as the extruder is starve-fed, the flow rate Q will remain unchanged while the hold up V decreases. Thus, the mean residence time $\bar{t}=V/Q$ will decrease with increasing screw speed. The starve-fed condition was ensured in our experiments by looking through the vent port window. The linear relation in (Fig.5.8) tells us that, within this operating range, the effective hold up is proportional to the screw speed.

From Fig.5.7 it can also be seen that mixing was improved by increasing the screw speed. This is because a higher screw speed causes a stronger stirring and, as explained previously, less hold up.

5.2.2 The Effect of Feed Rate

Fig.5.9 shows the normalized RTD curves for a set of experiments at various feed rates with all other operating conditions fixed (the screw speed was 300rpm). The corresponding mean residence times are plotted in Fig.5.10. It is clear from these plots that an increasing feed rate decreases the mean residence time and decreases the amount of mixing. The mean residence time – feed rate relation is not linear, and an exponential curve (the solid curve) fits the data better than

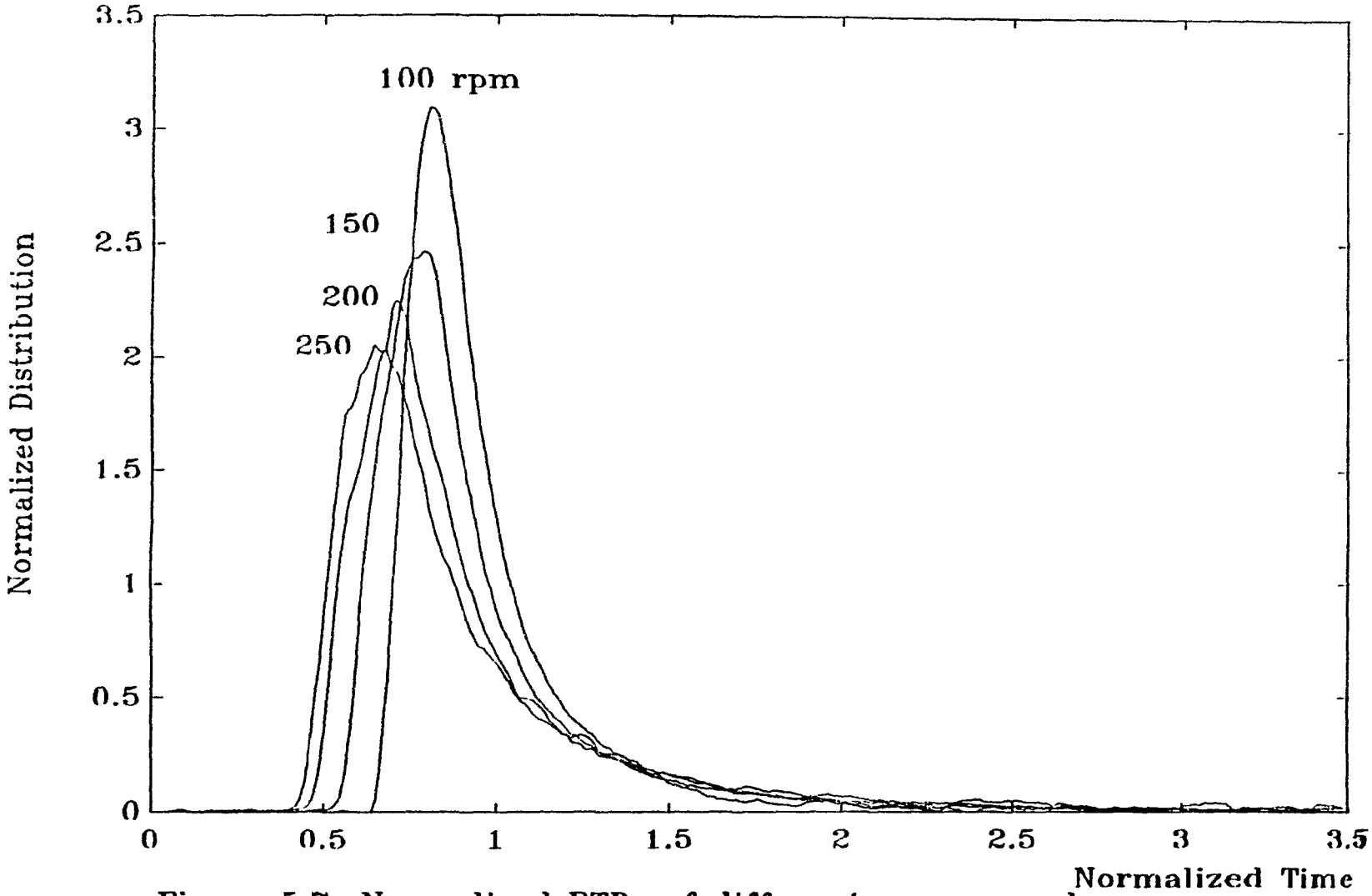

Figure 5.7 Normalized RTDs of different screw speed

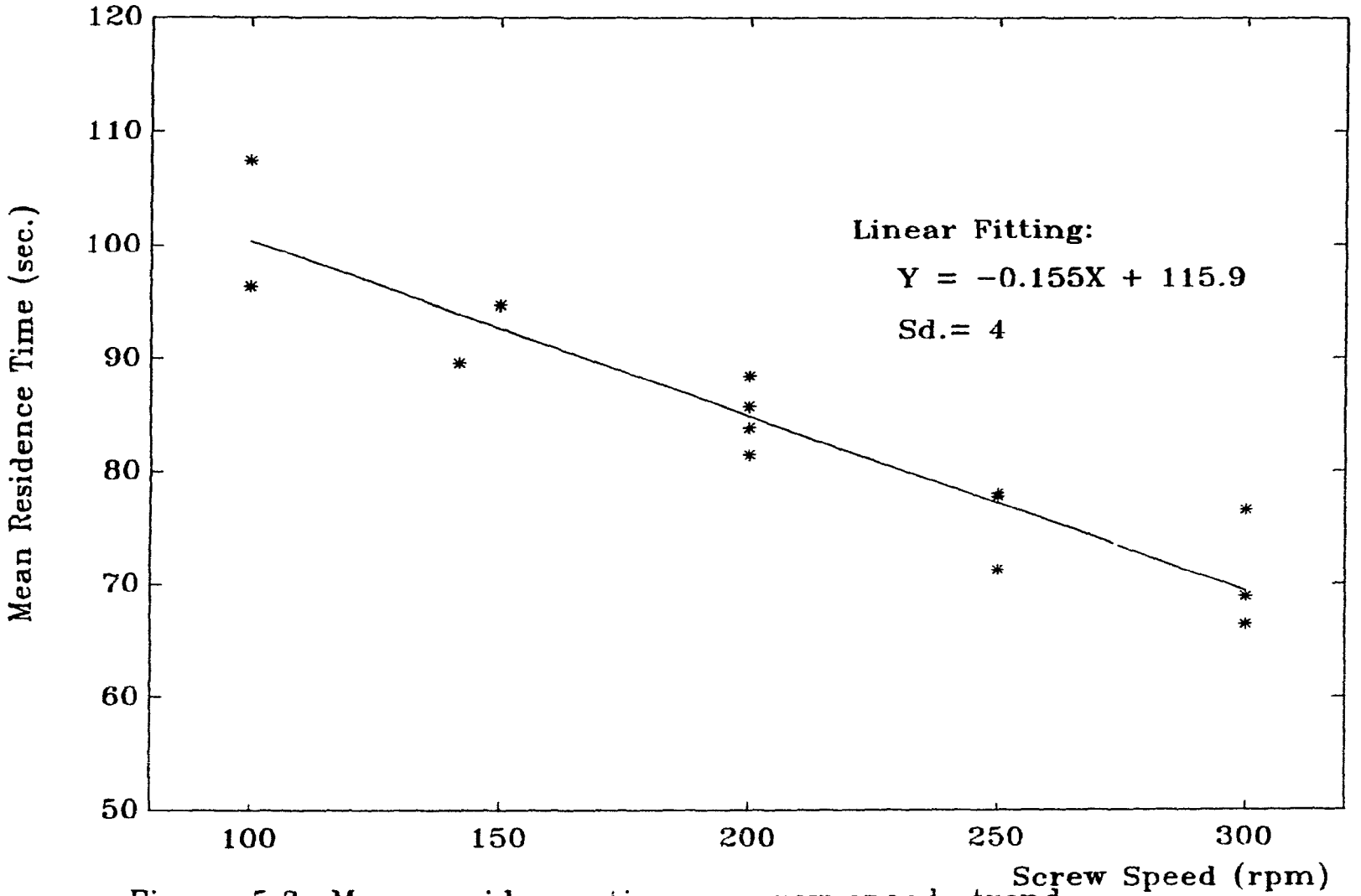

Figure 5.8 Mean residence time – screw speed trend

a straight line (the dashed line). This is to be expected since for a fixed hold up, V, we should have $\bar{t} \propto 1/Q$. While increasing Q also increases the effective hold up (which compensates for the decreasing of $\bar{t}$), the $\bar{t} - Q$ curve in Fig.5.10 is less concave than an inverse proportion relation.

Kao and Allison (1984) also studied the effects of the operating conditions on the mean residence time for a ZSK-30 extruder. Our results of both the screw speed trend and the feed rate trend are in general agreement with theirs except that, for the screw speed trend, they extended their experiments to a very high speed (492rpm at 4.5kg/hr) where the straight line curved and levelled out.

5.2.3 The Effect of Viscosity

The effect of viscosity on the residence time was studied both by increasing the screw barrel temperature and by using a lower viscosity material (melt index changed from 2 to 10).

Fig.5.11 shows two normalized RTDs with a 10°C difference in the barrel temperature profile. The screw speed was 200rpm, and the feed rate was 8kg/hr. At higher temperature (lower melt viscosity) we found a longer mean residence time and slightly worse mixing.

RTDs for two PP resins having different viscosities are compared in Fig.5.12. The screw speed was 250rpm, and the feed rate was 6kg/hr. It was found that the lower viscosity polymer

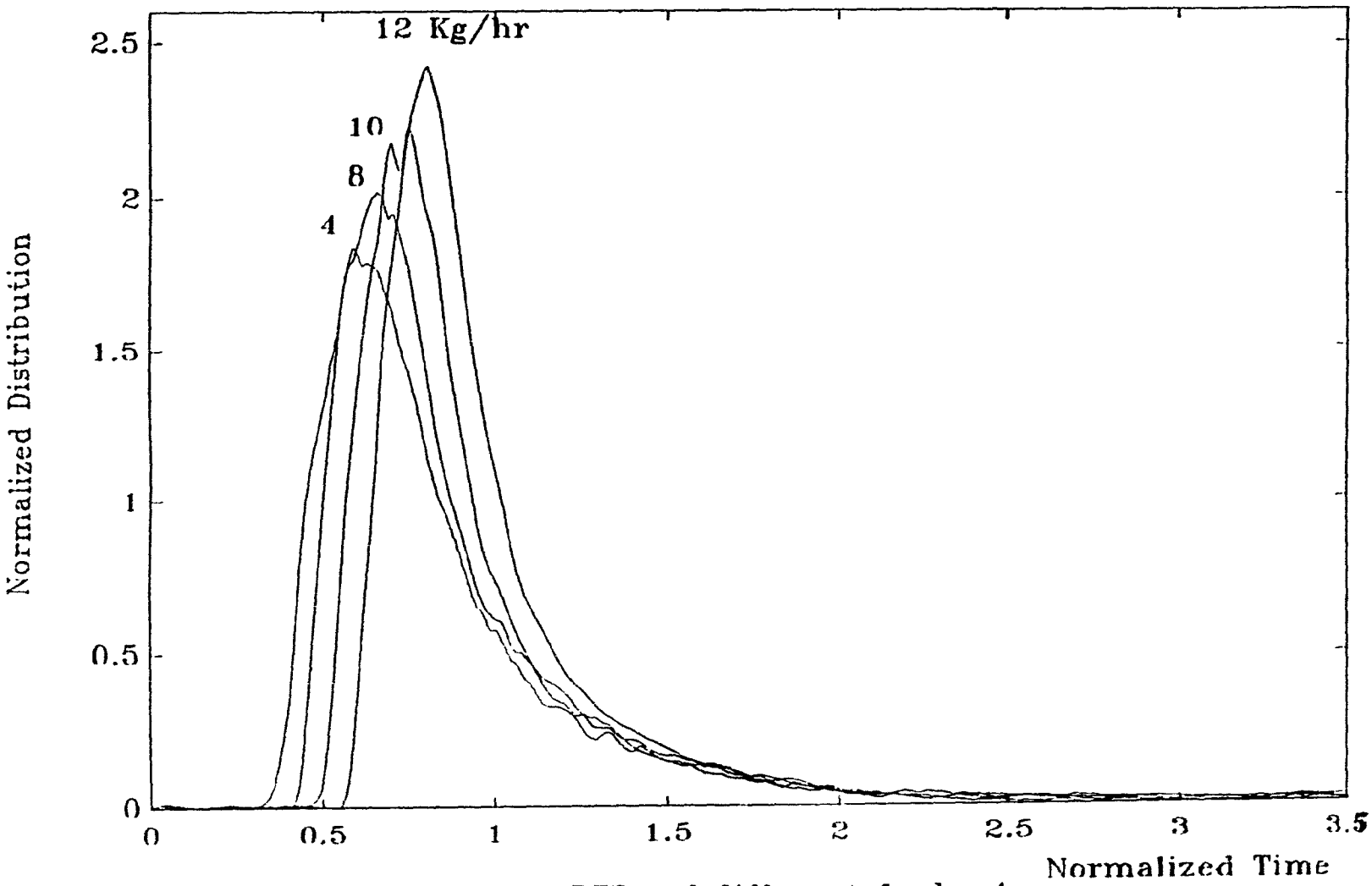

Figure 5.9 Normalized RTDs of different feed rate

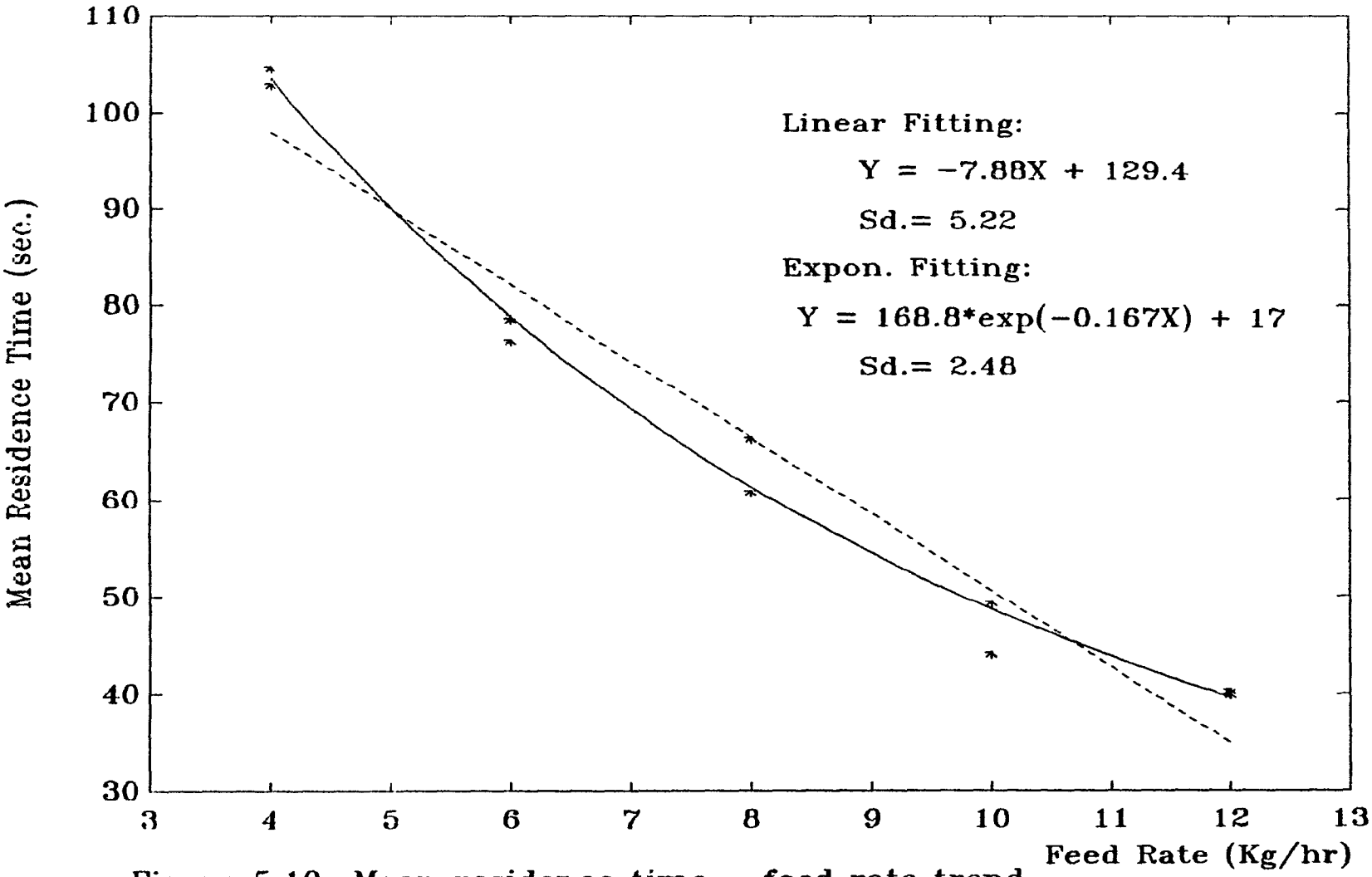

Figure 5.10 Mean residence time − feed rate trend

has a longer mean residence time, while the quality of mixing is almost the same (same effect as a higher temperature).

Kao and Allison (1984) reported that the barrel temperature profile had almost no effect on their mean residence times. Our results do not conclusively contradict this report since we did only a few comparative experiments, and the calculated mean residence time differences were small and of the same order as the error in our measurements.

5.2.4 The Effect of the In-line Rheometer

Some feed rate trend experiments were done with the McGill in-line rheometer installed (but without rotating its drum) in order to study the effect of the rheometer on the residence time. The screw speed was 300rpm. The resulting RTDs are plotted in Fig.5.13, and the corresponding mean residence times are shown in Fig.5.14. Comparing Fig.5.14 with Fig.5.10, we see that with the rheometer the fitted exponential curve becomes more concave and is shifted upward. This results from the additional flow volume (effective hold up) and flow resistance (increasing of back pressure) caused by the rheometer. When converted to mean residence time, there is a 80% increase at the points of 4kg/hr feed rate and a 85% increase at 12kg/hr feed rate. This is quite a large change especially when dealing with reaction extrusion process. It is suggested that in any future modification of the in-line rheometer the dead volume, which was about 91 cm^3, be reduced.

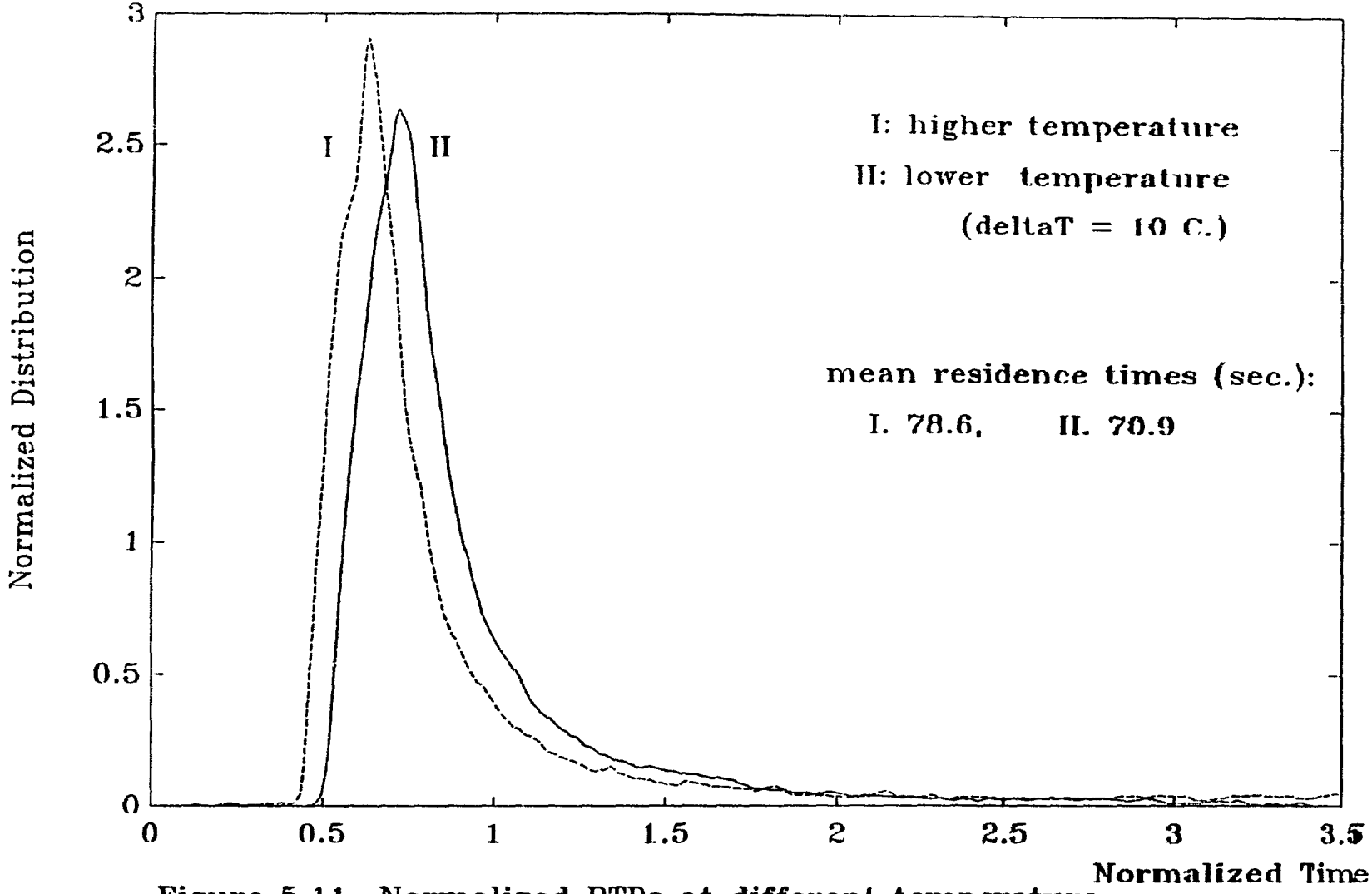

Figure 5.11 Normalized RTDs at different temperature

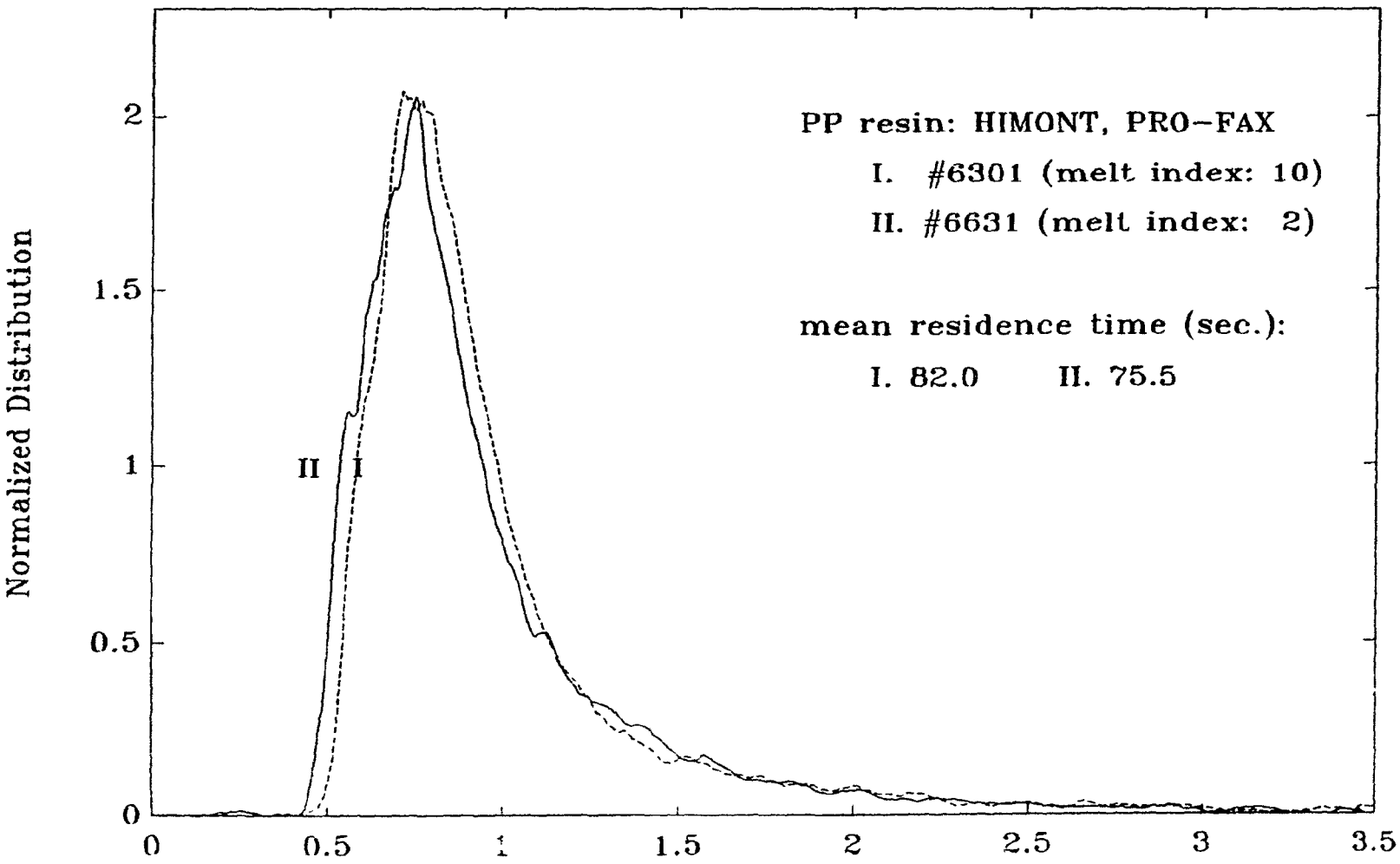

Figure 5.12 Normalized RTDs of different PP resins

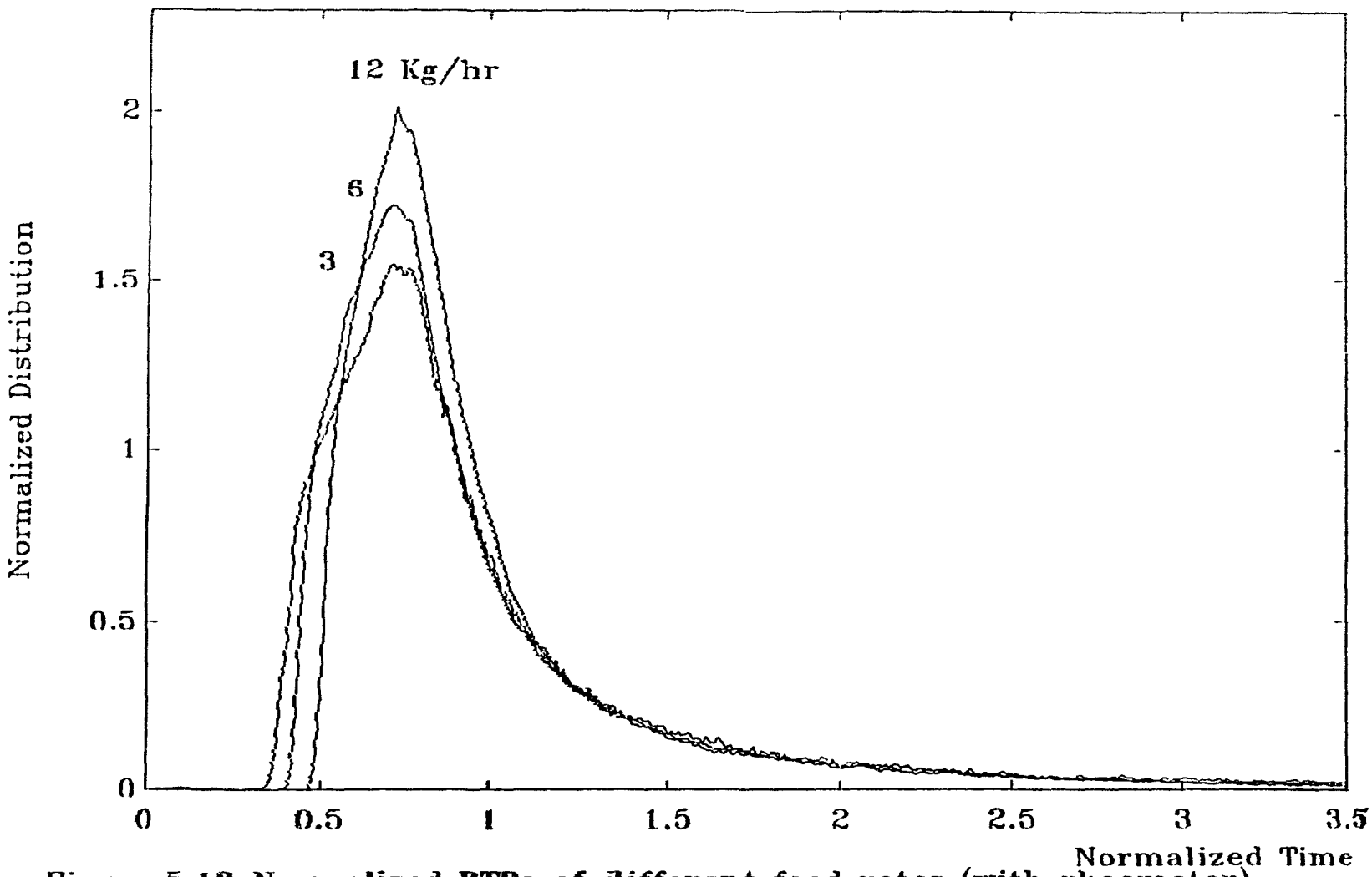

Figure 5.13 Normalized RTDs of different feed rates (with rheometer)

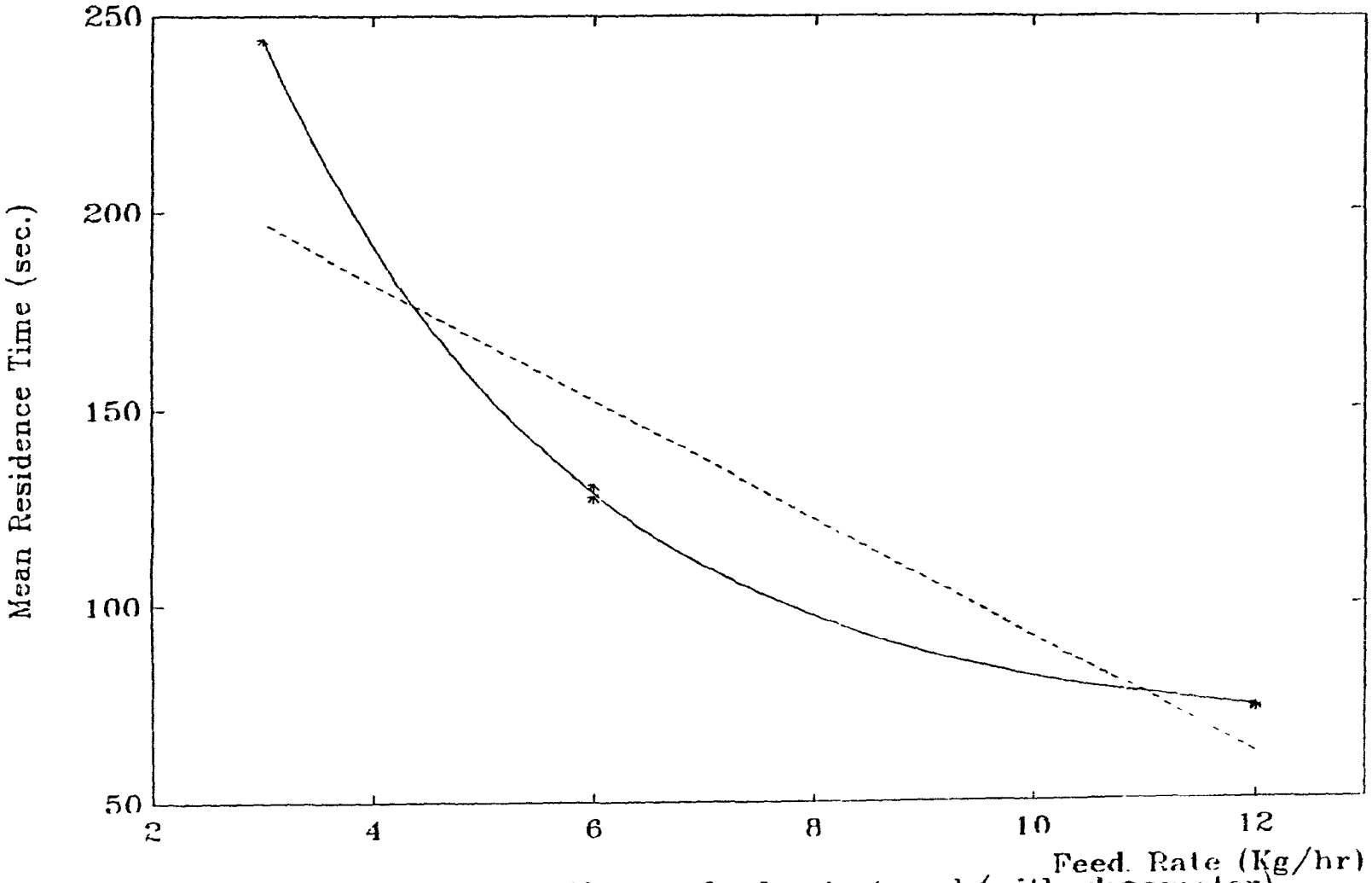

Figure 5.14 Mean residence time – feed rate trend (with rheometer)

CHAPTER 6 CONCLUSIONS AND RECOMMENDATIONS

6.1 Conclusions

From the experimental results and the discussions above, the following conclusions can be drawn.

1. The laser-photomultiplier optical method works well. Despite the non-uniformity problem in the sensor cell, it is still quite adequate for the precise determination of tracer concentration. Data collected from continuous on-line monitoring gives clear RTD curves with an estimated range of less than 6% of the mean residence time. Furthermore the method gives reproducible results.

2. When working with polypropylene under normal operating conditions, the Werner & Pfleiderer ZSK-30 extruder has a mean residence time ranging from 40 seconds to 100 seconds depending on operating conditions.

3. Increasing the screw speed or the feed rate shortens the mean residence time. The former causes better mixing while the latter causes worse mixing. Within a reasonable range, the mean residence time – screw speed relation is linear while the mean residence time – feed rate trend is nonlinear.

4. Lower viscosity material causes a longer residence time and worse mixing in the extruder, as does operation of a higher temperature. However, these viscosity effects are very weak, and more experimental runs are required to get the quantitative relations.

5. The in-line rheometer adds considerable residence time to the system. For the normal range of operating conditions, the mean residence time of the rheometer is comparable with that of the extruder itself. This has implications for future modifications of the in-line rheometer.

6.2 Recommendations

Although the optical method developed in this project works well, there is opportunity for further improvement. The following recommendations are made.

1. Add a mixer, probably stationary, upstream of the sensor cell to improve the uniformity of tracer in the extrudate. The mixer should give maximum mixing in the radial direction with minimum axial mixing. The mixer should be installed in the adapter flow channel to avoid adding additional residence time.

2. The non-uniformity of the tracer seen in the cell could be compensated by using a semiconductor photo-array in place of the photomultiplier. The photo-array elements would be placed normal to the flow as illustrated in Fig.6.1. Signals from each element, corresponding to the local light flux in that area, could be weighted and summed to indicate the instantaneous tracer concentration across the cross-section of the flow channel. The weighting would depend on the velocity profile.

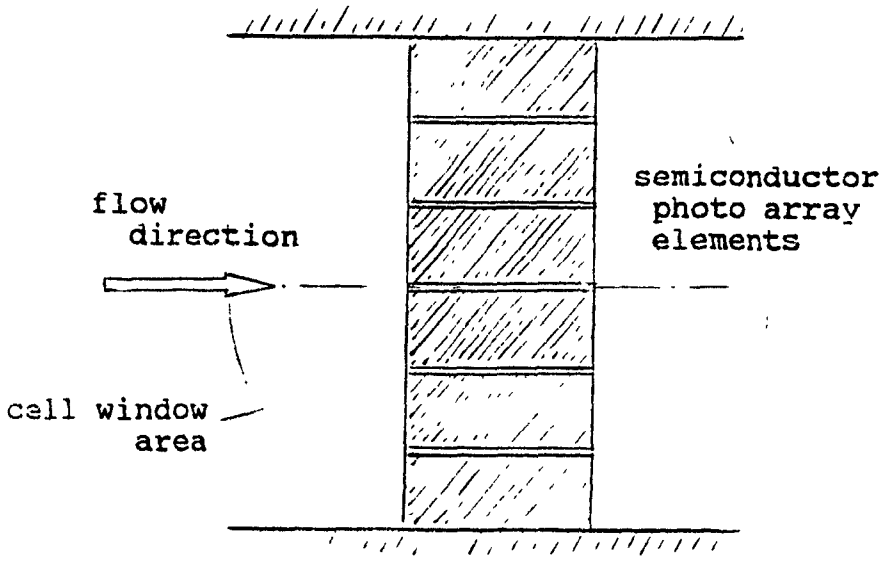

Figure 6.1 The semiconductor photo array

3. The magnetic tracer, with our modification (Section 3.2), is still an attractive method for on-line RTD measurement. One advantage is that it can be used with non-transparent polymers. However, in order to accomplish the on-line RTD measurements, a tracer preparation technique must be developed and the possible effect of temperature on the sensor coil must be considered.

REFERENCES

1. Bigg,D. and S.Middleman, "Mixing in a Screw Extruder. A Model for Residence Time Distribution and Strain", **Ind. Eng. Chem., Fundam., 13,** 66 (1974).

2. Bigio,D. and M.Wigginton, "Mixing in Twin Screw Extruders Under Starve-Fed Conditions", **6th Annual Meeting Polym. Proc. Soc., France,** p08-01 (1990).

3. Bounie,D., "Modelling of the Flow Pattern in a Twin-Screw Extruder Through Residence Time Distribution Experiments", **Journal of Food Engineering,** 7, 223 (1988).

4. Broadhead,T.O., "Development of an In-Line Rheometer for Control of Reaction Extrusion", **Ph.D. thesis**, Dept.Chem.Eng., McGill Univ.(1992).

5. Bur,A.J., C.L.Thomas, S.C.Roth, F.W.Wang, and F.M.Gallant, "Measurement Technology for Polymer Processing Based on Fluorescence Spectroscopy", **Soc. Plastics Eng. ANTEC, 36**, 1589 (1990).

6. Cassagnau,P., M.Bert, A.Michel, C.Mijangos,"An Ultraviolet Method for the Determination of the Residence Time Distribution in a Twin Screw Extruder", **Soc. Plastics Eng. ANTEC, 37**, 856 (1991).

7. Danckwerts,P.V.,"Continuous Flow Systems Distribution of Residence Times", **Chem. Eng. Sci., 2,** 1 (1953).

8. Dontula,N., G.A.Campbell, R.Connelly, J.Wenskus,"Degradation Study of HDPE Using Residence Time Distribution Analyses", 7th Annual Meeting Polym. Proc. Soc., 352 (1991).

9. Fenner,R.T., Extruder Screw Design, Iliffe, London (1970).

10. Golba,J.C., "A New Method for the On-line Determination of Residence Time Distributions in Extruders", **Soc. Plastics Eng. ANTEC, 26**, 83 (1980).

11. Gotsis,A.D. and D.M.Kalyon, "Simulation of Mixing in Co-rotating Twin Screw Extruders", **Soc. Plastics Eng. ANTEC, 35**, 44 (1989).

12. Herrmann,H., U.Burkdardt, and S.Jakopin,"A Comprehensive Analysis of the Multi-screw Extruder Mechanisms", **Soc. Plastics Eng. ANTEC, 23**, 481 (1977).

13. Janssen,L.P.B.M., Twin Screw Extrusion, Elsevier Scientific Publishing Company, London and New York (1978).

14. Janssen,L.P.B.M., L.P.H.R.M.Mulders, and J.M.Smith,"A Model for the Output From the Pump Zone of the Double Screw Processor or Extruder", **Plast. Polym., 43**, 93 (1975).

15. Janssen,L.P.B.M., R.W.Hollander, M.W.Spoor, and J.M.Smith, "Residence Time Distributions in a Plasticating Twin Screw Extruder", **AICHE Journ., 25**, 345 (1979).

16. Kao,S.V. and G.R.Allison, "Residence Time Distribution in a Twin Screw Extruder", **Polym. Eng. Sci., 24**, 645 (1984).

17. Kemblowski,Z. and J.Sek, "Residence Time Distribution in a Real Single Screw Extruder", **Polym. Eng. Sci, 21**, 1194 (1981).

18. Levenspiel,O., Chemical Reaction Engineering, 2nd ed., Wiley, New York (1972).

19. McKelvey,J.M., Polymer Processing, Wiley, New York (1962).

20. Meijer,H.E.H. and P.H.M.Elemans, "The Modelling of Continuous Mixers. Part I:The Co-rotating Twin-Screw Extruder", **Polym. Eng. Sci., 28,** 275 (1988).

21. Middleman,S., Fundamentals of Polymer Processing, McGraw Hill, New York (1977).

22. Mohr,W.D., R.L.Saxton, and C.H.Jepson, "Theory of Mixing in the Single-screw Extruder", **Ind. Eng. Chem., 49,** 1857 (1957).

23. Morton,D.H., Polymer Processing, Jones, New York (1989).

24. Nauman,E.B. and B.A.Buffham, Mixing in Continuous Flow Systems, John Wiley & Sons, New York (1983).

25. Nelson,B.I., "Use of an In-Line Rheometer to Control the Polypropylene Vis-breaking Process", **Ph.D. thesis,** Dept.Chem.Eng., McGill Univ. (1992).

26. Nichols,R.J., "Mixing Studies in Counter-Rotating, Tangential Twin Screw Extruders", **AICHE Meeting, Paper No.59f,** Washington, DC (1983).

27. Pearson,J.R.A., Mechanics of Polymer Processing, 2nd ed., Elsevier Applied Science Publishers, London and New York (1985).

28. Pinto,G. and Z.Tadmor,"Mixing And Residence Time Distribution in Melt Screw Extruders", **Polym. Eng. Sci., 10,** 279 (1970).

29. Potente,H. and H.Lappe, "Analysis of Residence Time

Distribution in Conventional Plasticising Extruders", **Plastics and Rubber Processing and Applications, 6**, 135 (1986).

30. Potente,H. and S.M.Schultheis, "Investigations of the Residence Time and the Longitudinal Mixing Behaviour in Counter-Rotating Twin Screw Extruders", **Intern. Polym. Proc., IV, 4**, 255 (1989).

31. Rauwendaal,C.J., Polymer Extrusion, Hanser Publishers, Munich (1986).

32. Sakai,T. and N.Hashimoto, "Experimental Study on the Comparison of Various Kinds of Twin Screw Extruder Characteristics", **6th Annual Meeting Polym. Proc. Soc.**, 04-kn1 (1990).

33. Schule,H., S.Meder, S.Stuttgart, and C.Muller, "Determining the Residence Time Behaviour in Extruders", **KUNSTSTOFFE German Plastics, 78, 1,** 26 (1988).

34. Shah,S., S.F.Wang, N.Schott and S.Grossman, "Counter-rotating Twin Screw Extruder as a Devolatilizer and as a Continuous Polymer Reactor", **Soc. Plastics Eng. ANTEC, 33**, 122 (1987).

35. Skoog,D.A. and D.M.West, Principles of Instrumental Analysis, Holt, Rinehart and Winston, New York (1971).

36. Stamato,H.J. and R.A.Weiss, "Determination of the Residence Time Distribution in a Plasticating Extruder Using an Ionomer Tracer", **Soc. Plastics Eng. ANTEC, 31**, 42 (1985).

37. Suh,N.P. and N.H.Sung, Science and Technology of Polymer Processing, MIT Press (1977).

38. Tadmor,Z. and C.G.Gogos, Principles of Polymer Processing, John Wiley & Sons, New York (1979).

39. Tadmor,Z. and I.Klein, Engineering Principles of Plasticating Extrusion, Van Nostrand Reinhold Co., New York (1970).

40. Todd,D.B., "Residence Time Distribution in Twin-Screw Extruders" **Polym. Eng. Sci., 15, No.6**, 437 (1975).

41. Todd,N.B. and H.F.Irving, "Axial Mixing in a Self-wiping Reactor", **Chem. Eng. Prog., 65,** 85 (1969).

42. Tzoganakis,C., Y.Tang, J.Vlachopoulos, and A.E.Hamielec, "Measurements of Residence Time Distribution for the Peroxide Degradation of Polypropylene in a Single-Screw Plasticating Extruder", **Journ. Appl. Polym. Sci., 37,** 681 (1989).

43. Werner,H. and K.Eise, "An Analysis of the Conveying Characteristics of Twin-Screw Co-Rotating Extruders", **Soc. Plastics Eng. ANTEC, 25**, 181 (1979).

44. White,J.L., Twin Screw Extrusion, Hanser Publisher, Munich and New York (1990).

45. White,J.L., S.Montes, M.H.Kim, Y.Wang, W.Szydlowski, "Modelling of Flow and Mixing in Modular Inter-meshing Co-rotating and Tangential Counter Rotating Twin Screw Extruders", **6th Annual Meeting Polym. Proc. Soc.**, 08-03 (1990).

46. Wolf,D. and D.H.White, "Experimental Study of the Residence Time Distribution in Plasticating Screw Extruders", AICHE Journ., 22, 122 (1976).

47. Wolf,D. and W.Resnick, "Residence Time Distribution in Real Systems", **I&EC Fundam., 2**, 287 (1963).

48. Wyman,C.E., "Theoretical Model for Intermeshing Twin Screw extruders: Axial Velocity Profile for Shallow Channels", **Polym. Eng. Sci., 15**, 606 (1975).

49. Zwietering,T.N., "The Degree of Mixing in Continuous Flow Systems" **Chem. Eng. Sci., 11**, 1 (1959).

NOTATION

A – the inner area of the coil, $A=\pi R^2$; absorbance

a – instrument constant

B – background signal of pure polypropylene absorbance

b – the width of the coil; the thickness of the absorber solution, or the depth of the sensor cell

C – concentration; molar concentration

C_i – tracer concentration in the ith material column under the sensor window

$C_{in}(t)$ – input tracer concentration

$C_{out}(t)$ – output tracer concentration

$C_{out}(t_i)$ – output concentration at the ith sampling time

D – axial dispersion coefficient

D/uL – vessel dispersion number used in Levenspiel's dispersion model

d – width of the sensor window in the flow direction

d_{in} – inner diameter of the coil former

e – end point of the base line of RTD curve

F(t) – cumulative residence time distribution function

f – frequency

f(t) – residence time distribution function; density function

$f_\theta(\theta)$ – normalized residence time distribution function

K – instrument constant obtained from the sensor calibration; relative permeability of the testing material

K_1 – relative permeability of the former material

K' – modified equivalent relative permeability

L – inductance; vessel length

L_i – coil number i

ΔL – inductance change of the sensor coil with and without the tracer sample inserted

l/d – aspect ratio of the magnetic tracer material

n – coil turns

P – back pressure in the metering zone of the extruder; intensity of the light received by the photomultiplier

P_B – intensity of background light passing through pure polypropylene

P_i – intensity of local light passing through the area S_i of the sensor cell window

P_o – intensity of the light source

Q – total volume flow rate, $Q=q_f-q_b$

q – volume flow rate

q_b – back flow rate

q_f – forward flow rate

R – outer radius of the coil former

r – inner radius of the coil former

S – slope of the V/C calibration curve in Figure 4.5; projecting area of the sensor cell window

S_i – projecting area of the ith column of the sensor cell window

s – starting point of the base line of a RTD curve

T – signal sampling period of the raw data, 0.3 second

t – time; residence time; effective time of the sensor

t_i – effective time of the ith column of the sensor

Δt – injection time where the pulse exists

$\bar{t}$ – mean residence time

u – velocity of the flow

u_i – velocity of the flow at the ith column

V – hold-up of the melt polymer inside the extruder; volume; the output voltage of the photomultiplier

V_B – background signal from the photomultiplier, the base line

V_0 – average of the beginning section of the $V(t_i)$ curve

$V(t_i)$ – recorded data (voltage) from the photomultiplier

$W(t)$ – washout function

X_L – inductive reactance

δ – small distance along the flow direction

$\delta(t)$ – Dirac delta function, impulse

ϵ – molar absorptivity of a material

θ – dimensionless time, $\theta=t/\bar{t}$

μ – permeability of the material under test

μ_0 – permeability of the vacuum

μ_n – nth-order moment of the residence time distribution, $\mu_1=\bar{t}$

τ – dummy variable of integration with units of time

APPENDIX 1 NONLINEAR SPATIAL AVERAGE AND EFFECTIVE TIME MEAN PROBLEM

Our optical method is based on Beer's law. There are some errors associated as with the use of this method to measure tracer concentration. These problems are discussed below.

I. Beer's Law and Concentration Measurement

A simple expression of Beer's law is that when light passes through a cell filled with a solution of light absorbers, the light absorbance is proportional to the concentration of the absorbers in the solution (Skoog, 1971). This is illustrated in Figure A.1, and Eq.1 gives the mathematical expression.

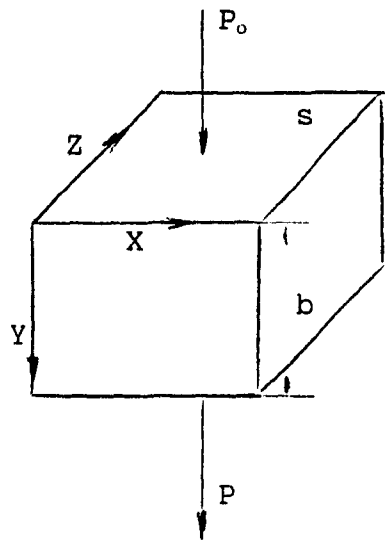

$$\log(P_o/P)=\epsilon bC=A \qquad (1)$$

Figure A.1 Illustration of Beer's law

Where S is the projected area, P_0 is the intensity of the

light source, P is the light intensity after absorbtion, $A=\log(P_0/P)$ is the absorbency, b is the thickness of the cell along the light direction (Y direction), C is the concentration (moles per litre) of the solution, and the parameter ϵ is the molar absorptivity of that absorber.

When a photomultiplier is used to detect the tracer concentration, it gives an output voltage signal, V, that is proportional to the light flux received:

$$V = aPS \qquad (2)$$

where P is the intensity of the light received, S is the window area (projecting area), and **a** is an instrument constant. Since for pure polymer there is still some absorbance, Eq.1 must be modified:

$$\log \frac{P_0}{P} = B + \epsilon bC \qquad (3)$$

where B is the background signal:

$$B = \log \frac{P_0}{P_B} \qquad (4)$$

and P_B is the background light intensity.
Substituting Eq.4 into Eq.3, we have:

$$\log \frac{P_B}{P} = \epsilon bC \qquad (5)$$

By using Eq.2, Eq.5 can be written in terms of voltage:

$$\log \frac{V_B}{V} = \epsilon b C \qquad (6)$$

$$or, \qquad \log \frac{V}{V_B} = K C \qquad (7)$$

where V_B is the base line of the RTD measurement (raw data), and K is a new instrument constant obtained from sensor system calibration. At a given time t, Eq.7 relates the photomultiplier output V(t) to the instantaneous tracer concentration C(t) and is thus the fundamental calculation formula in our RTD measurements.

Since Eq.6 is derived from Eq.2 and Eq.3, it requires a uniform distribution of the tracer particles over the entire projected area S, and the tracer concentration must be smaller than 0.01 mol. Both of these prerequisites are somewhat violated in the real case. This is illustrated next.

II. Nonlinear Spatial Average

The basic idea of RTD measurement is to continuously monitor the average tracer concentration across the cross section of the flow. For simplicity, we consider first a thin slice of the flow cell of thickness δ in the flow direction, as shown in Figure A.2. The flow is in the X direction and the laser light travels in the Y direction. The effective volume of the absorber is $w\delta b$ or Sb, where $S = w\delta$ is the projecting area. In the case of a uniform extrudate, Equation 5 or 6

holds for the entire effective volume. For the non-uniform case, this effective volume can be further divided into very small elements of equal volume, say n columns by m rows. Each element has a volume (S/n)(b/m), which is much larger than the tracer particle size but small enough such that the tracer concentration inside any of these elements can be considered as uniform.

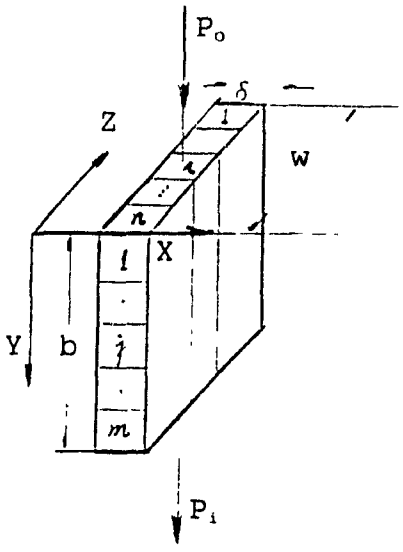

Figure A.2 Nonlinear spatial average

It is easy to prove from Beer's law that the logarithm of the signal is linearly additive along the Y direction (between rows). Thus the question is as follows: if the tracer concentrations are different in each column, is Equation 5 or Equation 6 still valid for the entire effective volume? The answer is no. To illustrate this, let us denote the projected area of the ith column as s_i (s_i=S/n), the tracer concentration in it as C_i, and the light intensity transmitted by that

column as P_i (as in Figure A.2). Then, by definition, we can write:

$$C = \frac{1}{n}\sum_{i=1}^{n} C_i \qquad (8)$$

$$P = \frac{1}{n}\sum_{i=1}^{n} P_i \qquad (9)$$

with ϵ, b, V_B, P_B unchanged (same as in the uniform case). Now, under the same intensity of light source, P_0, we apply Beer's law to each column:

$$\log\frac{P_B}{P_i} = \epsilon b C_i \qquad (10)$$

Thus, by combining Equations 8, 9, and 10, the overall concentration C can be expressed as:

$$\epsilon bC = \epsilon b\frac{1}{n}\sum_{i=1}^{n} C_i = \frac{1}{n}\sum_{i=1}^{n}\log\frac{P_B}{P_i} = \log P_B - \frac{1}{n}\sum_{i=1}^{n}\log P_i \qquad (11)$$

Comparing Equation 11 with Equation 5 we find that only when

$$\frac{1}{n}\sum_{i=1}^{n}\log P_i = \log P \qquad (12)$$

will Equation 5 still hold. Unfortunately this is not the case since generally:

$$\sqrt[n]{P_1 P_2 \cdots P_n} \neq \frac{1}{n}(P_1 + P_2 + \cdots + P_n) \qquad (13)$$

In other words, when the extrudate is non-uniform, the (logarithmic) linear relation (Equation 6 or 7) is no longer valid, and a nonlinear spatial average on the tracer concentration is required to calculate the overall tracer concentration in the effective volume.

III. Effective Time Mean

The analysis in Section II was applicable to a thin cross section, i.e., the slice had a very small thickness ($\delta \to 0$). For a practical sensor cell, however, the window must have a finite length in the flow direction in order to have a reasonable sensitivity and to reduce the noise. Therefore, the actual signal is an integration involving many such thin layers. An integration over time is used instead of over distance in the following discussion, since it is easier to illustrate the problem in the time domain.

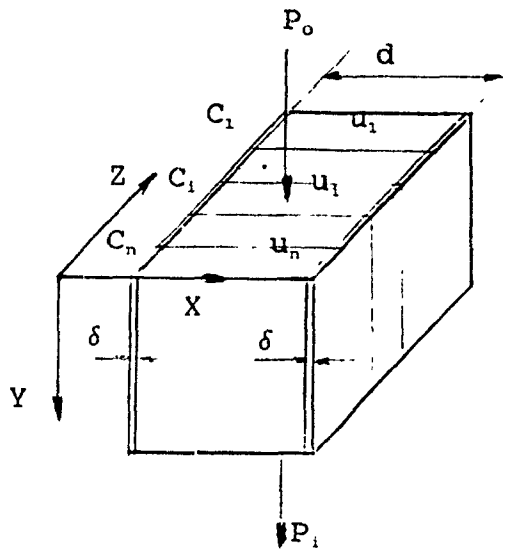

Figure A.3 Effective time problem

Figure A.3 shows an effective volume similar to that in Figure A.2 except that the thickness is now **d**, which is much larger than δ. For simplicity let us first assume that the material in each column in Figure A.2 has a uniform concentration (C_i for the **i**th column), and a uniform velocity (u_i for the **i**th column). Suppose that at time t=0 these material columns were at the left edge of the effective volume in Figure A.3, while at $t=t_i$, the **i**th material column reaches the right edge. Then the contribution of the tracer in the **i**th column to the signal is:

$$\int_0^{t_i} C_i dt = C_i t_i \qquad (14)$$

where the effective time $t_i=d/u_i$. It is easy to see that in plug flow (Figure A.4.a), where $u_1=u_2=\ldots=u$, a parallel window gives a uniform effective time for all the material columns, and the tracer concentrations in them are thus equally weighted (excluding the nonlinear spatial average problem discussed before).

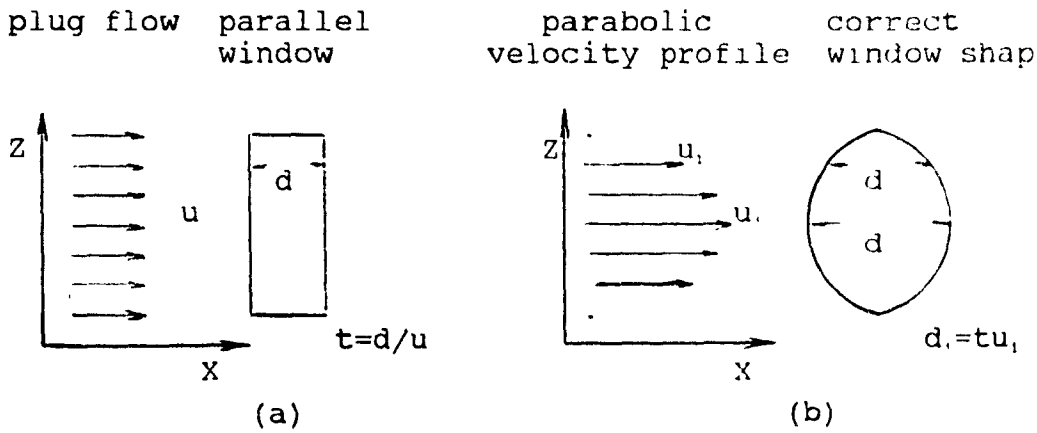

Figure A.4 Effective time mean

However, for fully developed laminar flow, the velocity of each column is different and hence a non-parallel window is required. As shown in Figure A.4.b, the window width, d_i, at each position (Z_i) must be calculated individually as $d_i=tu_i$, where u_i is the local velocity, and t is the desired signal integration time. The actual situation is more complicated than this, since there are also the quartz walls at the top and the bottom of the effective volume in Figure A.3 so that the u_i is not uniform but a function of Y.

Beside the problems discussed in II and III above, there is also a possible violation of Beer's law caused by the non-uniformity of the tracer concentration. Since even when the overall tracer concentration of the entire effective volume is sufficiently low, the local tracer concentration may go beyond the limit of Beer's law.

APPENDIX 2 RAW-DATA DISKETTE

There is a ASCII file named README.ASC on the diskette describing the data and the programs it contained.

KAO®

Mini-Floppy Disks From The Surface Scientists
Mini-disques souples, produits par les spécialistes des surfaces
Mini-Disketten von Oberflächenbehandlungsspezialisten